VARIATION IN SEDIMENT AND GEOCHEMISTRY AS EVIDENCE OF CHANGES IN FLOWPATHS TO A KARST SPRING IN SOUTHEASTERN PENNSYLVANIA

A Thesis
Submitted
to the Temple University Graduate Board

In Partial Fulfillment
of the Requirements for the Degree of
Master of Science

By
Jennifer H. Tancredi
May 2004

Laura Toran
Dr. Laura Toran, Thesis Advisor

David E. Grandstaff
Dr. David E. Grandstaff

Dr. Dennis O. Terry, Jr.

ABSTRACT

The purpose of this study was to determine whether the pathways through which groundwater travels in a karst aquifer change between seasons and during storm events. A specific goal was to determine how these pathways affect the water chemistry and sediment in the discharge from a karst spring.

From July 2002 through December 2003, storm and continuous monitoring data were collected from Nolte Spring, a former community water supply in southeastern Pennsylvania. Storm samples were collected using an automatic sampler. Additional samples were collected by hand during site visits performed on a bi-weekly to monthly basis. All samples were analyzed for suspended sediment and ions. Datalogging sensors were installed in the spring for the entire study period to record stage, conductivity and temperature.

A conceptual model for the study spring was devised to describe storm response and seasonal changes in terms of recharge and groundwater flow pathways. The stage and conductivity at baseflow varied during the study period, as characterized by two end-members. The drought end-member was characterized by low stage and high conductivity. Frequent snowmelt and rain led to high stage and low conductivity during the flood end-member. The relatively high conductivity observed at times during the study period is indicative of slower groundwater flow paths to the spring. Storm responses were determined by different pathways based on recharge type, which was classified as point or diffuse recharge, based on the mean storm intensity. Point recharge events are caused by high intensity storms ($\geq$1.5 cm/day) and the storm response was an

initial increase in conductivity followed by a decrease. Diffuse recharge events are caused by low intensity storms ($\leq$ 1.5 cm rain/day) and snowmelt, and the response was a decrease in conductivity.

Geochemistry and sediment mineralogy were also affected by the flow pathways. During the drought, the P_{CO2} was the lowest of the monitoring period, indicating outgassing from dewatered conduits. The SI_C was slightly above saturation, and calcite was observed in the sediment samples, indicating possible calcite precipitation. In the growing season of 2003, P_{CO2} was the highest of the monitoring period, due to increased recharge and plant activity. Calcite was also observed in the sediment collected during this time. Various calcite morphologies suggest dislodging of calcite particles from the wall rock and transport of precipitated calcite from another area of the karst aquifer or the soil-bedrock interface as possible reasons for the existence of calcite in the spring. During Winter and early Spring 2003 the suspended sediment mineralogy was mostly siliciclastics such as clays and silt. Sediment concentrations in Nolte Spring were lower than expected, possibly due to the absence of stagnant conduits in the karst aquifer where sediment would accumulate and be flushed during storms.

The karst system feeding Nolte Spring has characteristics of both conduit and matrix/fracture flow. Specifically, calcite undersaturation points to conduit flow, whereas stable temperature and low coefficient of variation of hardness (CV) points to matrix/fracture flow. The results of this study also reveal the importance of long-term continuous monitoring, which shows the changeable nature of the karst aquifer in terms of storm water pathway and spring response.

ACKNOWLEDGEMENTS

I am deeply grateful to my entire family, including my parents, Dolores and Nick Tancredi, and my sister, Laura for their love, encouragement, and unending support throughout this program and all the years before. I would like to thank Kyle Margiotta for his love, understanding and support, which included lending his illustration talents to some of the figures in this thesis. I would also like to express my appreciation and respect for my advisor, Dr. Laura Toran, for the opportunity to work on this project and her guidance throughout. Her dedication to her students and to the science of hydrogeology has inspired me greatly, and she has helped me to cultivate a love of research and the desire for quality science, which will last throughout my career. This project was made possible by funding provided by the National Science Foundation NSF/EAR Hydrology Program, NSF Award 0125601.

I would like to express my gratitude to Ellen K. Herman of the Department of Geosciences at Penn State University, who I consider a second advisor, for performing all of the SEM analyses for this study and her insightful feedback and guidance over the past two years. I am also thankful for the opportunity to have worked with her advisor, William B. White, whose pioneering work in the field of karst science helped make this study possible, and for his invaluable advice and comments. Appreciation is also extended to Maria Klimkiewicz and Nichole Wonderling of the Materials Characterization Laboratory at Penn State University, for their assistance in the SEM and XRD analyses.

Many thanks to Robert "Bucky" Buckwalter of the West Earl Township Water Authority for granting access to the study site, and for sharing with me both his knowledge of the site and his hip waders. Thanks also to John Diehl and Mike Moore, of the Pennsylvania Department of Environmental Protection, for background information on the study area.

Thanks are also due to the entire faculty, staff, and students of the Department of Geology at Temple University, for making my experience at Temple University positive and rewarding. Special thanks to my committee members, Dr. David E. Grandstaff and Dr. Dennis O. Terry, for their insightful comments, expertise lent to this study in their respective fields, and for their inspiration and encouragement. I would also like to thank Donald Deigh-Kai and Roger Cutitta of the Department of Geology at Temple University for their logistical support, which often included finding just the right square pegs for the round holes I gave them, and also Shelah Cox, both for administrative and moral support. Thanks also to my fellow graduate students, especially Terefe Mazengia, John Peake, and Danielle Target (office-mates and field partners extraordinaire), and also Patti Jannett, whose friendship and support from my first few days in the department to the last few weeks I will always cherish. Much of my research would not have been possible without the efforts of the following undergraduate workers over the last two years, many of whom were volunteers in the field and lab: Julie Acton, Kathy Gross, Ken Hayes, Heather Landherr, Szilvia Mathe-Puckey, Cecilia Mejias, John Petriello, Erin Pinder, Bryan Rillstone, Rebecca Roth, and Stephen Scott.

TABLE OF CONTENTS

LIST OF TABLES

LIST OF FIGURES

CHAPTER 1
INTRODUCTION

Karst aquifers are formed largely by the surface and subsurface dissolution of carbonate rock. Karst is characterized by undulating surface topography, sinkholes (often direct conduits from the surface to the aquifer), caves, springs, and "sinking streams" (Figure 1-1). These features require combination of concepts from both surface and groundwater hydrology in order to effectively study and understand karst aquifers (White, 1999).

Purpose

The purpose of this study was to test the hypothesis that the pathways through which stormflow travels in a karst aquifer to a spring affect the nature of chemical variability and sediment content in the discharge. Samples, water quality, and hydrologic measurements were collected between July 2002 and December 2003 at a spring in southeastern Pennsylvania to examine the changes in water chemistry and sediment concentration in the discharge from a karst spring between seasons and during storm events in order to determine the degree of variability in water chemistry and sediment concentration. Storm monitoring was conducted to determine if the geochemical variability and sediment observed provided clues to different flow paths through the karst.

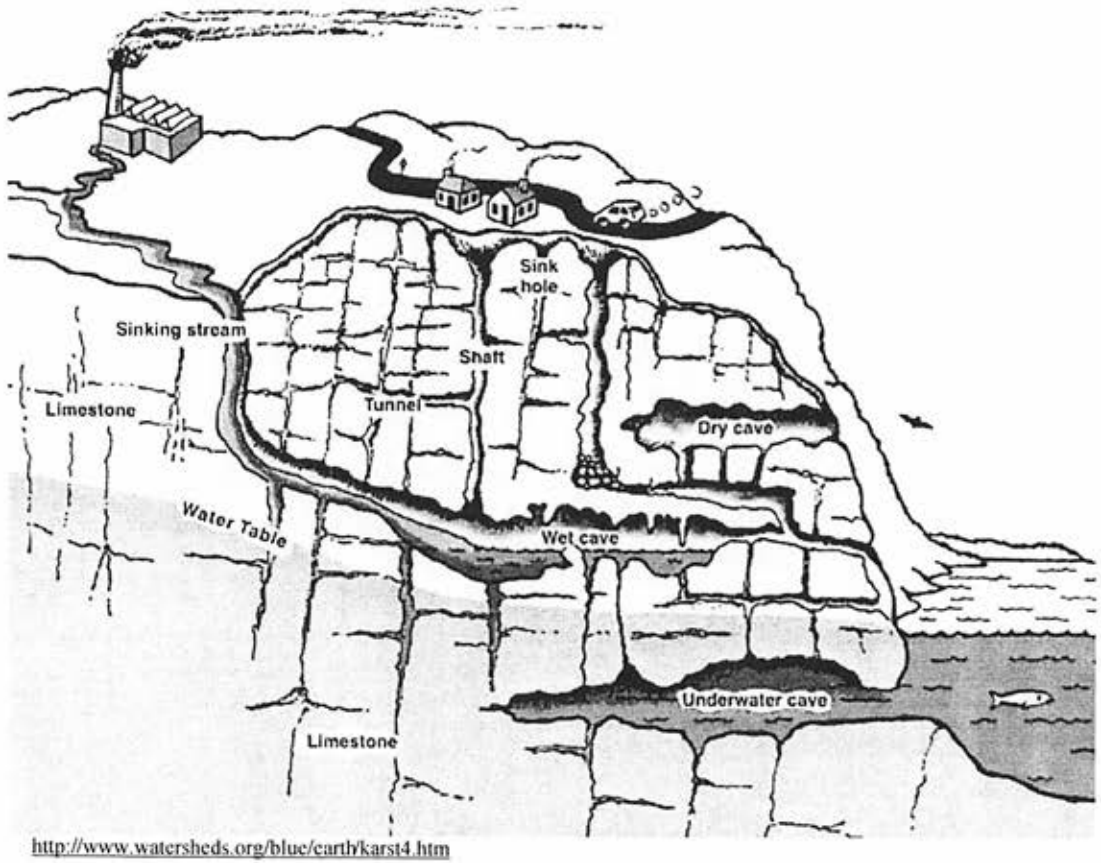

Figure 1-1. A karst aquifer and associated surface features. The system depicted here is larger than the karst system that is believed to feed Nolte Spring, but the concept of different groundwater flow pathways illustrated here is the same for a smaller karst system such as Nolte Spring.

Importance of Problem

Karst aquifers are an important source of potable water, as they supply drinking water to an estimated 25% of the world's population (Ford and Williams, 1989). They are also more susceptible to pollution than other aquifers, primarily due to the following factors: thin soils, which are poor filtering agents and allow rapid infiltration from the surface; lack of granular texture, which inhibits mechanical filtration as a self-purification process; short residence times and rapid travel times, which provide less time for biodegradation and natural attenuation of contaminants and enable contamination in karst aquifers to travel long distances (White, 1988).

A greater understanding of the chemical variability, hydrology, and sediment transport in karst aquifers is crucial to an accurate assessment of contaminant transport within a karst aquifer (Vesper and White, 2003; Mahler et al., 1999). Suspended sediment can be a contaminant (Ryan and Meiman, 1996; Mahler et al., 1999), and it is influential in the fate and transport of many other contaminants. In porous aquifers, sorption of contaminants to the immobile solid phase retards transport. Transport of contaminants by colloids (particles between 0.01 and 10 μm in size, with a high specific surface area; Drever, 1988) has been considered in fate and transport models, but in karst aquifers, sediment of many different sizes can be mobilized and act as a vector for contaminant transport, especially for compounds with low solubilities, such as metals, hydrocarbons, and pesticides (Mahler et al., 1999). Ryan and Meiman (1996) noted in their study of groundwater quality in Mammoth Cave National Park that the increase in suspended sediment following a storm event was concurrent with an increase in fecal

coliform bacteria, which indicates that suspended sediment may carry bacterial contaminants or that similar flow conditions mobilize both sediment and bacteria (Figure 1-2).

Because of the high variability in concentrations of sediment, water chemistry and hydrologic parameters during storms, it is important to be able to sample at the correct intervals and locations in order to accurately characterize the hydrologic properties of an aquifer and any contamination that may exist (Farmer and Williams, 2001). To this end, springs are excellent monitoring points for karst aquifers, as it is difficult to drill monitoring wells to intersect the proper conduit(s), while springs can be an outlet for an entire network of conduits (Farmer and Williams, 2001 citing Quinlan and Ewers, 1985). The importance of high frequency, flow-dependent sampling to determine water quality in the aquifer during baseflow and stormflow conditions has also been recognized (Ryan and Meiman, 1996). An understanding of the variability in the water chemistry and sediment of the discharge from a karst spring between seasons and in response to storm events will facilitate the development of a monitoring plan for karst aquifers to accurately characterize the spring during both storm and baseflow conditions.

Karst Hydrology

One way in which karst aquifers differ from porous or other fractured-rock aquifers is the heterogeneous flow paths. Karst aquifers contain three types of permeability, identified as matrix, fracture, and conduit flow (White, 1999). Matrix permeability is intergranular flow within the carbonate rock, whereas fracture permeability occurs along joints and bedding planes that may have been widened by dissolution. Conduits are "pipes", which

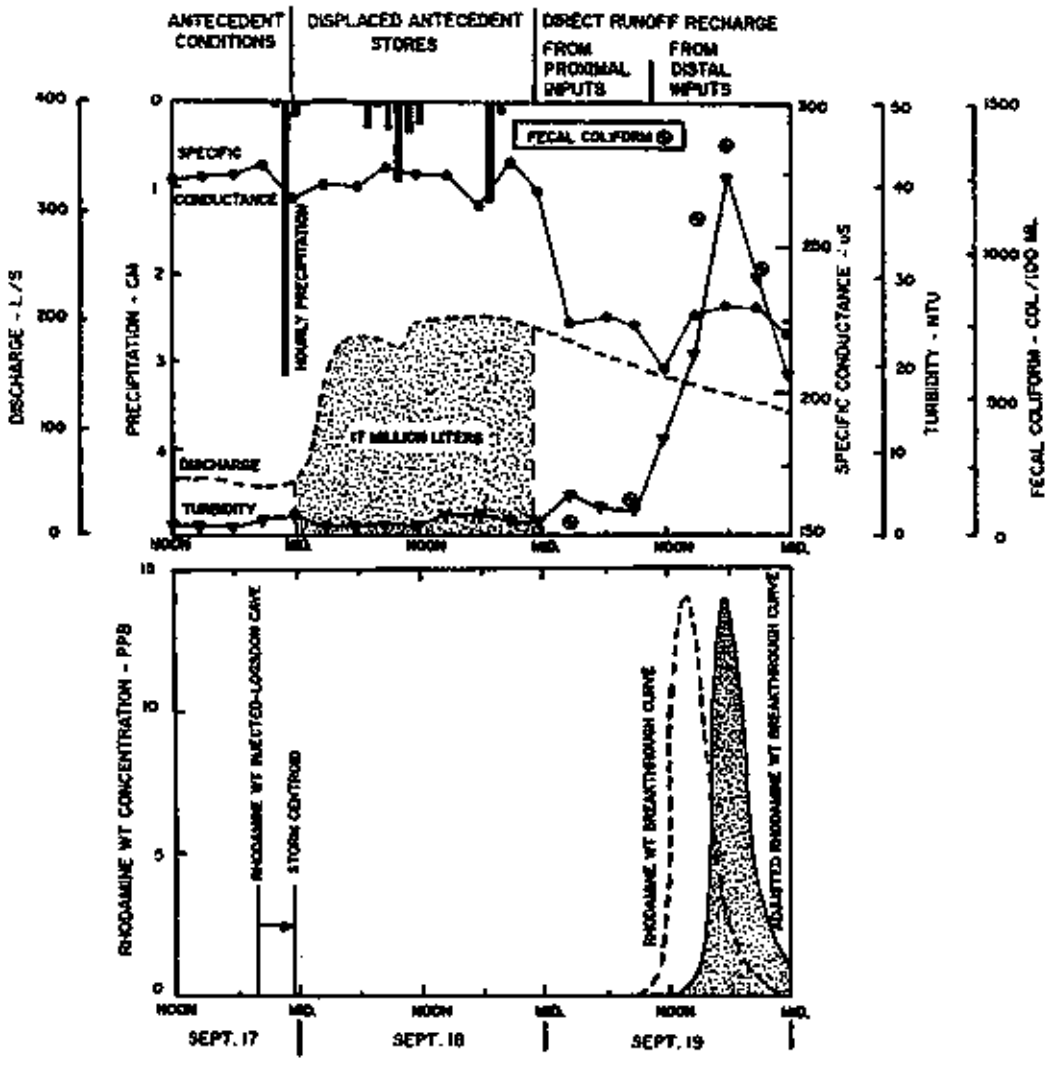

Figure 1-2. Water quality changes in discharge from Big Spring in Mammoth Cave NP, from Ryan and Meiman (1996). The fecal coliform increase is coincident with the turbidity maximum, indicating that suspended sediment may carry bacteria. However, coliform bacteria are similar in size to colloidal particles, so the bacteria may be transported separately.

have been significantly widened by dissolution along partitions in the carbonate rock and range from 1 cm to 30 or 40 m in size (White, 1999) (Figure 1-3). Conduit flow is complicated by turbulent, non-Darcian flow regimes, which dominate at widths greater than 1 cm. Most aquifers are a mix of all three flow-types, with either matrix/fracture or conduit flow as the dominant type (White, 1988).

For karst aquifers in which flow occurs predominantly through a network of conduits, the travel times and directions for groundwater flow can be hard to characterize. Travel times in karst can be many times less than in a porous or fractured-rock aquifer over the same distance. Also, flow direction can be difficult to determine in a karst aquifer. All groundwater ultimately flows downhill, but groundwater flow paths in a karst network can be divergent or convergent. Water from one source in the groundwater basin may emerge from many outlets in various locations, or the discharge from a particular spring may be composed of a mixture of many conduits converging.

Recharge to a karst aquifer is also different because it may be stored temporarily in the vadose zone or enter rapidly through conduits. Storage occurs in the carbonate matrix, in vadose conduits, or in the epikarst, which is defined as the region in the upper weathered layers of rock at the base of the soil horizons, lying above the permanently saturated (phreatic) zone (Lakey and Krothe, 1996 citing Mangin, 1974). The epikarst is different from the soil or unsaturated carbonate rocks in that karstification occurs in this zone, which affects the chemistry of the water that is stored there (Vesper and White, 2003). The source of recharge to karst aquifers can be precipitation falling directly onto the karst surface or runoff from neighboring non-karst catchments which enters the

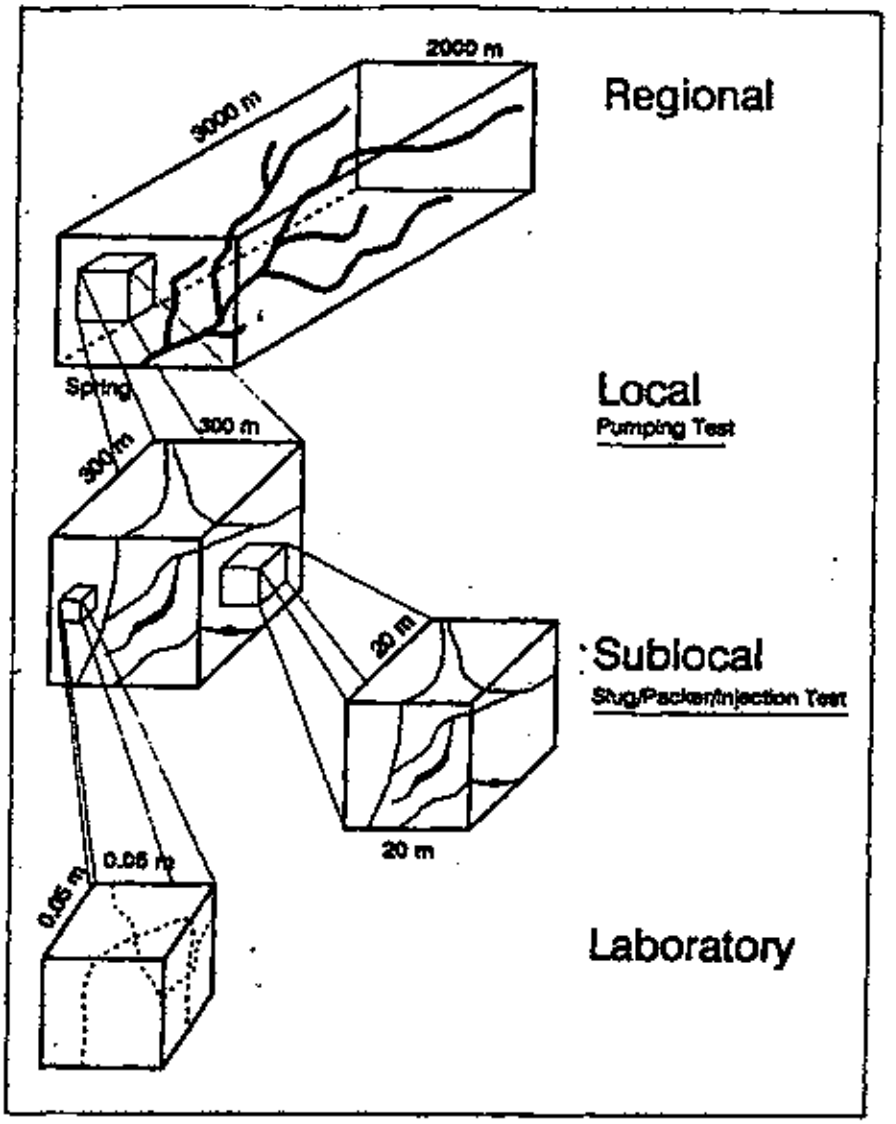

Figure 1-3. Scale dependence of karst aquifer permeability, from White (1999) citing Sauter (1992). Conduit permeability operates on a regional and local scale, while fracture permeability is on a local or sublocal scale, depending on the size of the fractures. Matrix permeability can be observed on a laboratory scale. Nolte Spring is probably fed by flow through small conduits or enlarged fractures.

aquifer through sinkholes, caves, or sinking streams. These different modes of recharge affect the geochemistry and hydrographs of storm discharge.

Previous Work on Karst Flow Paths

Exploration and Tracers

A variety of methods can be employed to map the karst network and try to determine the hydrologic pathways for a karst aquifer system. In large karst networks, with caves and large conduits, this has been accomplished using human exploration (White, 1988). Geophysical studies have also been successful in locating some larger karst features, such as cavities and conduits (Ford and Williams, 1989; Jenkins, 1999), but smaller conduits and fractures are more difficult to map.

For hydrologic studies of a karst system, some kind of tracer is necessary to determine the direction and rate of flow from a surface input to a monitoring point. There are a number of synthetic tracers, including dyes and other colorless chemicals, which are used for this purpose. In karst water investigations, fluorescent dyes are the most commonly used tracers (Smart, 1989 citing Smart and Laidlaw, 1977). Of these, the red fluorescent dye Rhodamine WT or Fluorescein, a yellow fluorescent dye, are the most often used, because they are stable and have a low natural background (Smart, 1989). Through examination of the shape and integral area under the breakthrough curve of the tracer, information may be obtained regarding the geometry of the conduit system, in addition to travel time and general flow direction (Smart, 1989 citing Smart and Ford 1982).

Natural Tracers and Geochemical Indicators

Additionally, natural tracers can be used to determine the source of discharge from a spring or determine different sources of recharge to the aquifer. These natural tracers include dissolved ions and natural isotopic tracers, which include isotopes of carbon, oxygen, and hydrogen (Lakey and Krothe, 1996; Katz et al., 1997). Dissolved ions, specifically calcium, magnesium and bicarbonate, are typically present in large concentrations in karstic waters. Although these ions are non-conservative, they can be used to identify different sources of recharge to an aquifer and to distinguish storm water from pre-storm water in spring discharge (Dreiss, 1989; Desmarais and Rojstaczer, 2002).

Chemical variability between springs and between seasons in a given spring may be used to draw some distinctions between the feeder systems of springs. The higher degree of variability is different from that of other types of aquifers. These variations in chemistry are due to the rapid throughput of recharge in karst systems (Dreiss, 1989). In most aquifers, the chemistry of the groundwater is a result of water-rock interactions, which operate over long periods of time. The slow rate at which these reactions proceed homogenizes the chemistry of the water so that it is constant over seasons, and does not change in response to storms. The close connection of karst groundwater to the surface can cause the chemistry of the water discharged from the spring to vary according to seasons, in response to storm events, or according to the pathway through which a particular volume of water travels through the karst network to the spring (Desmarais and Rojstaczer, 2002). These variations can occur as rapid changes in water quality

parameters such as pH, temperature or conductivity of the water, and in concentrations of dissolved ions or contaminants in groundwater.

Shuster and White (1971) used the chemical composition of discharge from a number of springs combined with field observations of topography within spring catchments to classify springs as either flowing from matrix-dominated feeder systems or conduit feeder systems. The springs in their study, which were all in generally the same area and hydrogeologic environment, showed a great deal in variation with respect to their seasonal chemographs. The springs classified as conduit-fed systems showed more of a response to seasonal changes than those classified as diffuse springs. Additionally, the conduit springs were the most undersaturated with respect to calcite and had the lowest hardnesses, yet the most variability in hardness. One of the springs, which was classified as diffuse-fed due in part to its high mean hardness, also exhibited a relatively large variability in hardness and was more undersaturated in calcite than the other diffuse springs. It was postulated that the feeder system for this spring might consist of poorly-developed conduits or a network of solutionally-widened fractures.

Isotopic tracers can also indicate the pathways of the water in the aquifer when compared to regional values for atmospheric water (Lakey and Krothe, 1996). Isotopes present in the water molecule itself include ^{16}O and ^{18}O, ^{2}H, and H or light hydrogen. Under low temperature conditions, the amounts of these isotopes only change as a result of physical processes such as diffusion, dispersion, mixing, and phase changes (Lakey and Krothe, 1996 citing Fritz et al. 1976; Toran, 1982). The conservative behavior of these isotopes makes them useful as tracers, to help determine the movement of water

masses and mixing between them (Lakey and Krothe, 1996), although tritium is generally used to determine the age of the water. Two of the isotopes of carbon, ^{12}C and ^{13}C, are present in the dissolved inorganic carbon species in the water, $HCO3^-$, CO_3^{2-}, and H_2CO_3 (Toran, 1982). The use of natural isotopes in karst groundwater investigations can be helpful in determining the pathways through which the water flowed, as the differences in the isotopic composition of spring water may indicate that discharge at one time has flowed through different formations than it did at another time (Katz et al. 1997).

Suspended sediment is another component of spring discharge that may be used as a natural tracer. Sediment transport in karst is often more similar to surface water systems than to other aquifers. Large pore diameters and turbulent, high-velocity flow enables transport of sediment larger than colloid-size (Mahler et al., 1999), and keeps particles suspended. The amount of spring discharge has been found to be the primary factor influencing the transport of larger (>4 - 5 μm) particles in karstic aquifers (Mahler et al. 1999). Discharge can also regulate the large suspended particle content in an aquifer, so that the distribution of particle sizes in spring discharge can be used to describe the prevailing hydrodynamic conditions in a karst system (Atteia and Kozel, 1997).

Chemical Variability During Storms

Changes in the chemistry of a spring in response to storm events have been studied extensively to determine the input from pre-event water and event water to the spring discharge before, during and after a storm (Dreiss, 1989; Ryan and Meiman, 1996; Lakey and Krothe, 1996; Desmarais and Rojstaczer, 2002; Vesper and White, 2003).

Dreiss (1989) used a two-component mixing model to describe the inputs of pre-event (baseflow) and event (quickflow, stormflow) water to the discharge from two karst springs in Missouri. In this model, concentrations of dissolved calcium and magnesium in samples were used to discriminate between the two components, baseflow and stormflow. At the time of peak discharge in response to a storm, it was determined that the primary contribution to spring discharge was pre-storm water, which had been displaced from the conduits by the more dilute storm water (Figure 1-4).

Lakey and Krothe (1996) used the stable isotopic composition of discharge at a spring in Indiana over the course of two storms to separate the storm hydrograph into pre-event and event water. Their results over the course of the storms occurred as a hysteresis curve, rather than points plotting along a tie line between two end-members. The deviation from the tie line between rainwater and phreatic water (pre-event water residing in the conduits) indicates that the contributions of rainwater and pre-event water to the storm discharge at their study site cannot be described by a simple mixing model. Additionally, the results of Lakey and Krothe's (1996) hydrograph separation show that the peak storm discharge is primarily composed of phreatic, pre-event water, while the largest contribution of event water is not discharged at the spring until 18-24 hours after the hydrograph peak (Figure 1-5). Lakey and Krothe interpreted these results to mean that the "old" phreatic water must be displaced before the "new" event water can be discharged through the spring. Ryan and Meiman (1996); Desmarais and Rojstaczer (2002); and Vesper and White (2003) observed similar examples of this "flushing" phenomenon during storms.

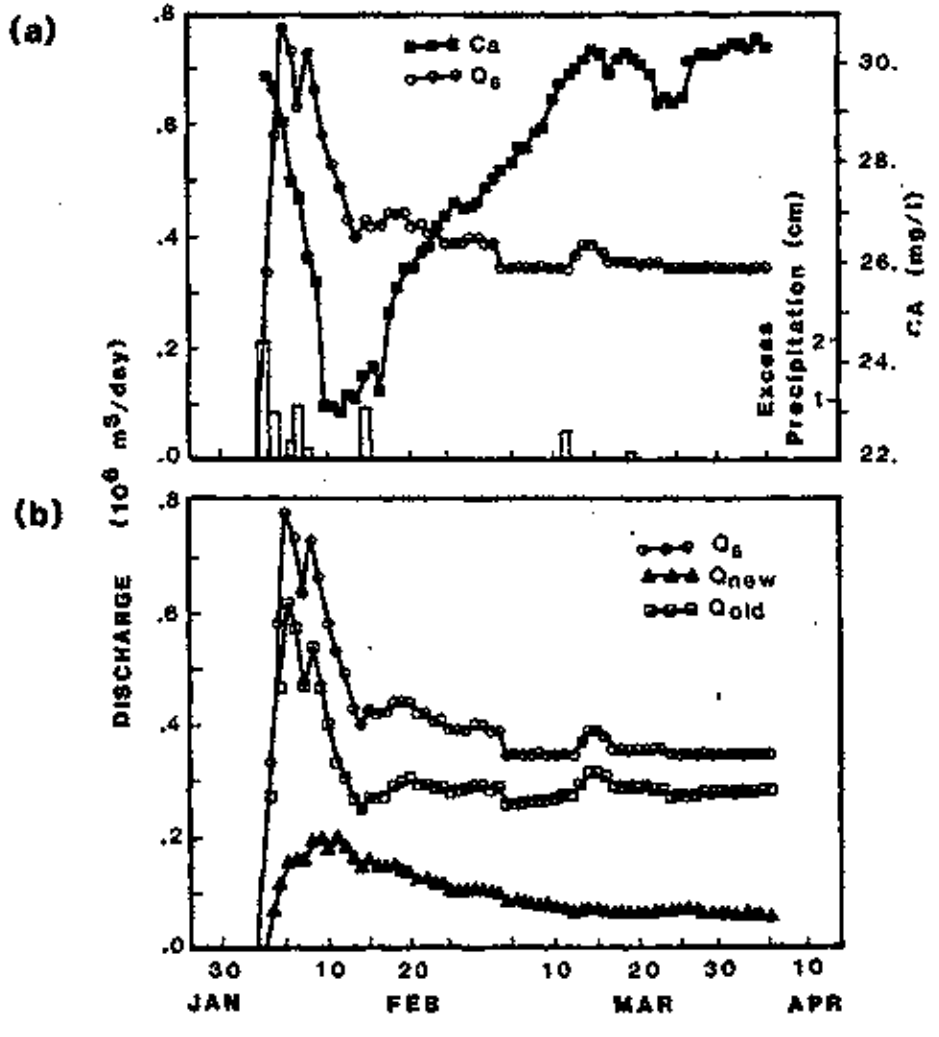

Figure 1-4. Storm response of Maramec Spring, February through April 1986, from Dreiss (1989). Dreiss used concentrations of dissolved Ca to differentiate old (pre-storm) water from new storm water. The hydrograph separation in (b) shows that the largest contribution to spring discharge is from the pre-storm water.

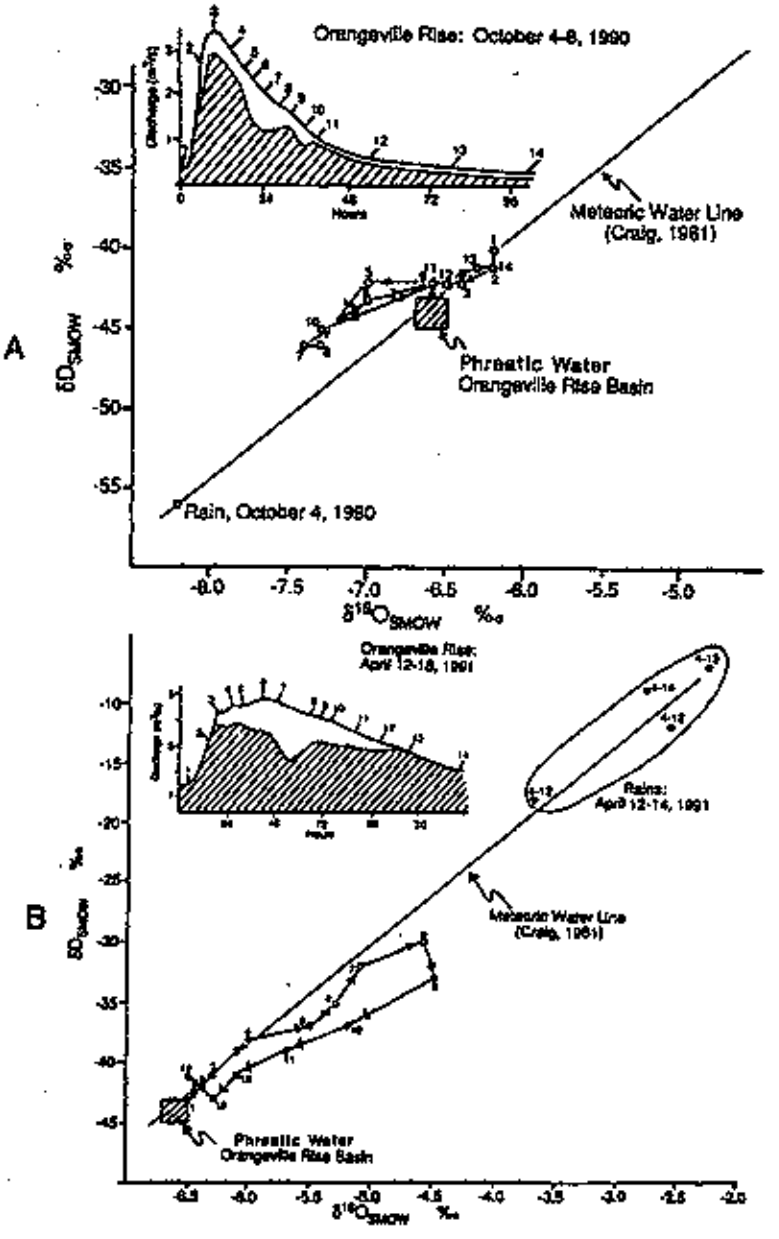

Figure 1-5. Hydrograph separation and progression in deuterium and oxygen isotopic composition during two storm monitoring periods at Orangeville Rise in Indiana, from Lakey and Krothe (1996). At peak discharge, the largest contribution appears to be from the pre-storm water, indicating displacement by storm water.

The usefulness of isotopes as tracers for the separation of a spring hydrograph into baseflow and stormflow can be limited by the requirements that the chemistry of the water entering the aquifer be distinct from the pre-event water in the aquifer and that the event water is uniform in both space and time (Dreiss, 1989). In these cases, it is necessary that the dissolved ion concentration be used instead. The major ion composition of precipitation is usually significantly lower than that of carbonate groundwater (Dreiss, 1989), especially with respect to the Ca^{+}, Mg^{+} and HCO_3^{-} ions. Dissolved ion concentrations, for which conductivity may be used as a surrogate, have been used in various studies as a natural conservative tracer to determine whether the pathways of water discharged from the spring differ seasonally (Shuster and White 1971; Dreiss, 1989) and among different storms (Desmarais and Rojstaczer, 2002).

During a storm event, Farmer and Williams (2001) observed a 60-fold increase in chloroform over pre-storm concentrations in the discharge from a contaminated karst spring in Tennessee. This increase in chloroform, a constituent present in the spring before the storm, but in smaller concentrations, lagged the conductivity minimum and peak discharge. The lag between the conductivity minimum and the concentration increases in other constituents, such as sediment, fecal coliform, dissolved CO_2, and some ions have been noted in other karst aquifers (Ryan and Meiman, 1996, Lakey and Krothe, 1996; Desmarais and Rojstaczer, 2002) (Figures 1-2, 1-4, and 1-5).

The high variability in the groundwater chemistry of karst aquifers is not only the result of surface water flowing through the karst network. Groundwater discharging from a spring can be from multiple sources within the underground karst network. Some of

these sources, vadose and epikarst storage, have been discussed above. Lakey and Krothe (1996) attributed the deviation of their stormflow isotopic composition from the Meteoric Water Line to contributions from pre-event water stored in the vadose zone and epikarst. Katz et al. (1997) identified a deep flow zone of old groundwater mixing with that of shallower conduits in samples from several municipal wells in the deeper parts of the Upper Floridan aquifer. Desmarais and Rojstaczer (2002) developed a conceptual model for a spring on the Oak Ridge Reservation in Tennessee which included the mobilizing of older, deeper residential water from smaller fractures and pores by "newer" recharge to the aquifer, resulting in the increase of the slope of the conductivity curve for the spring which they observed within one hour following the most intense portion of the storm event (Figure 1-6). Vesper and White (2003) examined the changes in P_{CO2} and $SI_{calcite}$ over the course of a storm in two springs in Kentucky, and found that the sources of recharge differ more at different times during a storm than they vary between different springs.

Site Description

Location

The study site is Nolte Spring in West Earl Township, Lancaster County, Pennsylvania (Figure 1-7). Nolte Spring is located approximately 4.5 meters in elevation above and about 90 m north of Conestoga Creek, a tributary of the Susquehanna River, which is in the Chesapeake Bay Watershed Area (John Diehl, Pennsylvania Department of Environmental Protection (PADEP), personal communication, 1992). The topography and land around the stream is gently rolling pastureland, while land use in the general

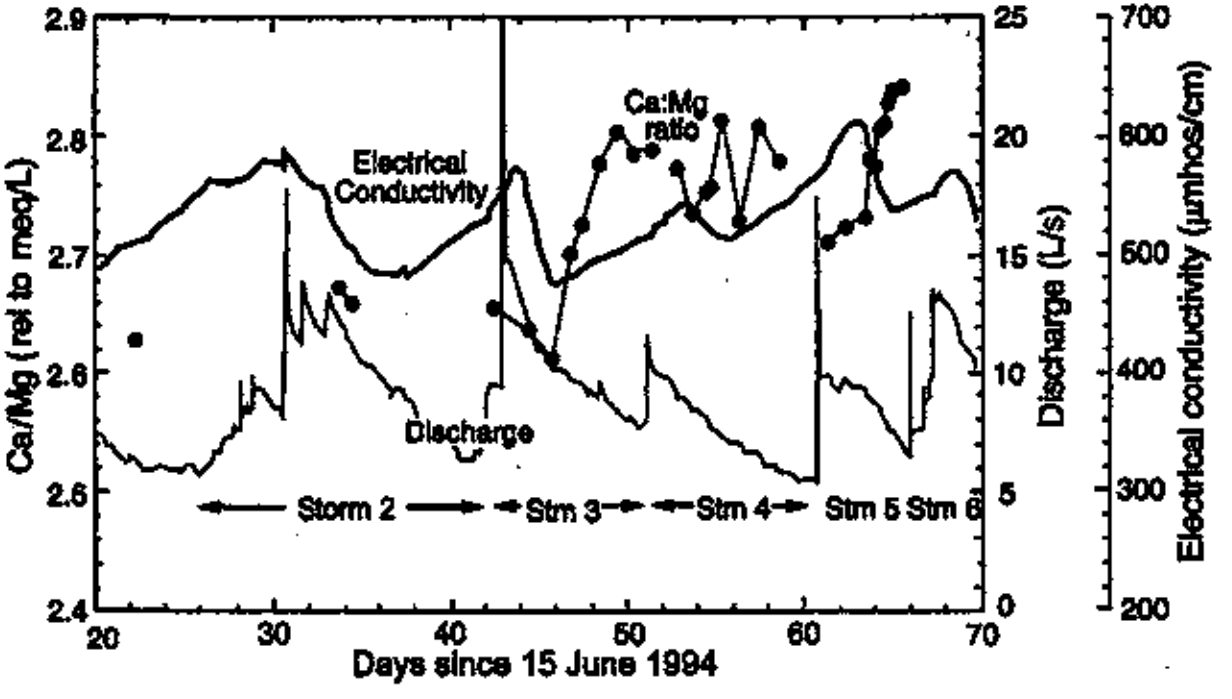

Figure 1-6. Discharge, conductivity, and Ca:Mg ratios in spring SS-5 in Oak Ridge, Tennessee from Desmarais and Rojstaczer (2002). The variability in Ca:Mg ratios between storms indicates different types of source water for each storm, depending on the characteristics of the storm and the antecedent conditions.

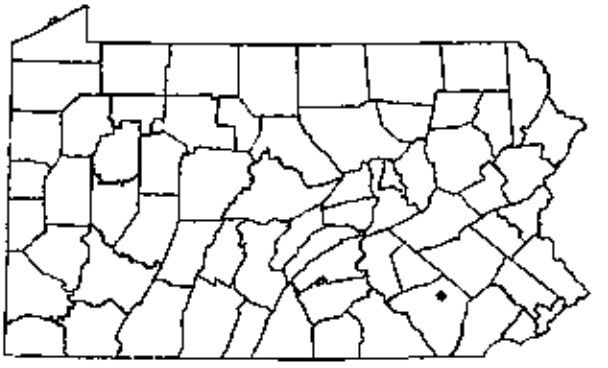

Figure 1-7. Location of study area. Nolte Spring (indicated by the red dot) is located in West Earl Township, in northeast Lancaster County.

area of the spring is a combination of agricultural, residential, commercial and some industrial. The spring run flows southwest from the spring mouth into a small tributary to the Conestoga Creek, which originates further north of Nolte Spring.

Regional Geology

The groundwater basin for Nolte Spring is comprised of the Beekmantown Group, which is early Ordovician in age. Adjacent to the basin is the Cocalico Shale which unconformably overlies the Beekmantown Group and is located north of the basin. The region lies within the axis of a broad synclinal valley. The contact between the Beekmantown Group and the Cocalico Shale occurs approximately 2 kilometers north of the spring (John Diehl, PADEP, personal communication, 1992; Poth, 1977). The Beekmantown Group is described as finely laminated limestone and dolomite (Jonas and Stose, 1926). It has been divided into several formations, the Stonehenge, Epler, and Ontelaunee Formations (Poth, 1977) (Figure 1-8). A fourth formation of the Beekmantown Group, the Rickenbach Formation, occurs in neighboring Berks and Lebanon Counties between the Stonehenge and Epler Formations, but is not found in Lancaster County (Meisler and Becher, 1971).

Local Geology

According to geologic maps of the area, Nolte Spring is underlain by the Epler Formation (Figure 1-9). Contacts with the Stonehenge Formation can be found nearby, within 0.4 kilometers to the northeast and less than 0.1 kilometers to the south of the spring, within the capture zone calculated for the spring, which is discussed in Chapter 3 (Kochanov, 1990). The Epler Formation has the most varied lithology of the formations

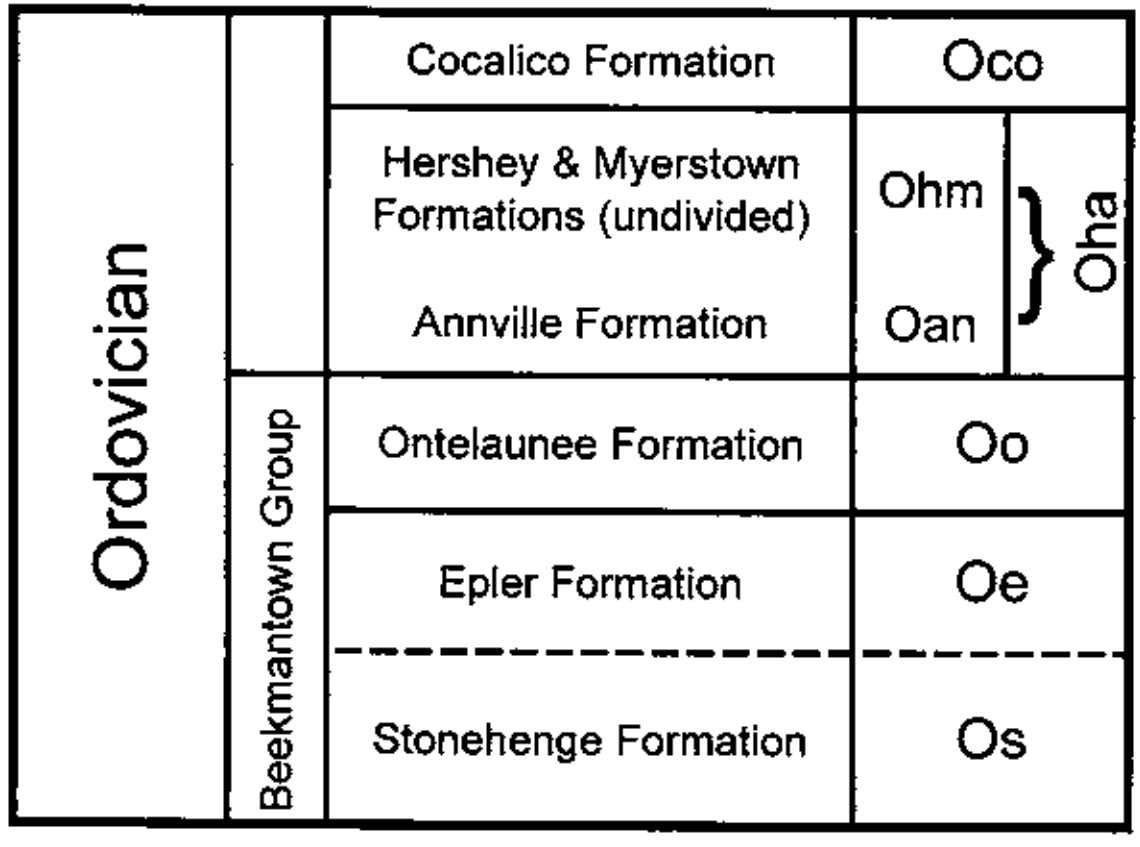

Figure 1-8. Stratigraphic column for the Ephrata Quadrangle. Nolte Spring is located in this quadrangle. In the vicinity of the spring, there is an unconformity between the Cocalico Shale and the interbedded limestones and dolostones of the Beekmantown Group.

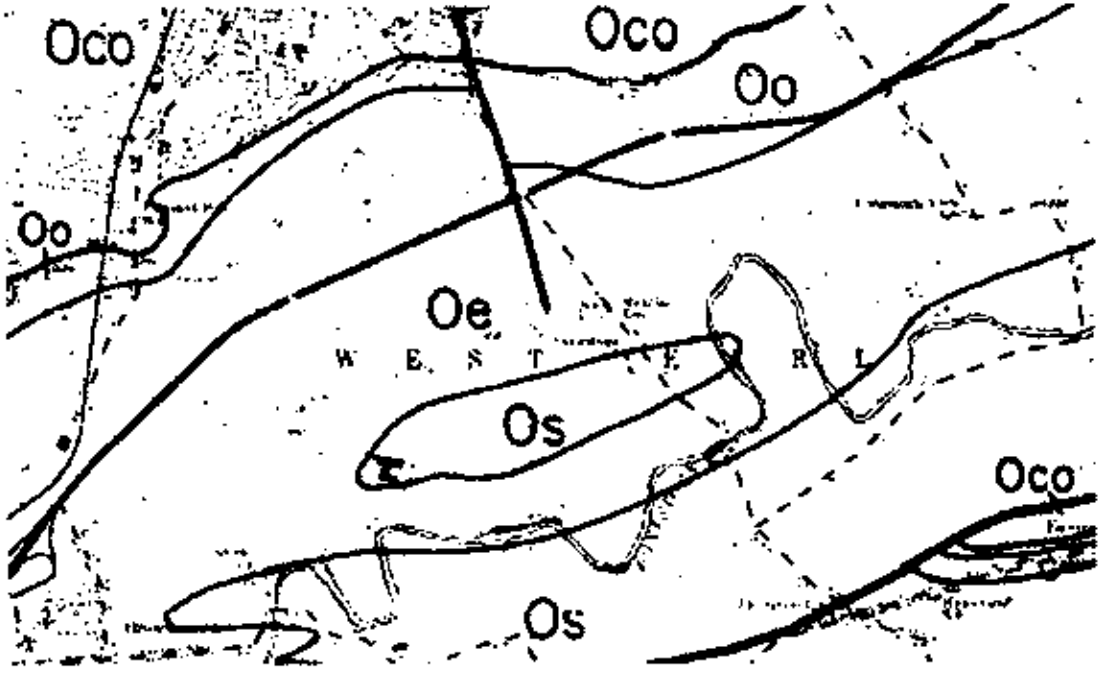

Figure 1-9. Local geology of study area. The spring (shown by the red dot) is close to the unconformable contact between the Stonehenge Fm. (Os) and the Epler Fm. (Oe). The Ontelaunee Fm. (Oo), another member of the Beekmantown Group, and the Cocalico Shale (Oco) are to the north. (From Berg and Dodge, 1981)

in the Beekmantown Group, but in general, it consists of intervals of interbedded limestone and dolomite. Both pure limestone and dolostone are present, including all combinations of these rock types (Meisler and Becher, 1971). The thickness of the Epler Formation is between 6,100 to 7,600 meters (Meisler and Becher, 1971). The Stonehenge Formation is described as a medium gray to medium dark gray, very finely to finely crystalline limestone, often with dark-shale laminae and calcarenite beds. It is estimated to be 1,500 to 3,000 meters thick (Meisler and Becher, 1971). The Stonehenge Formation has been described as the highest-yielding carbonate-rock formation in the Lancaster 15-minute quadrangle by Meisler and Becher (1971), with a mean specific capacity of 25 liters per second per meter (lps/m) (121 gpm/ft) and a median specific capacity of 3.6 lps/m (17.5 gpm/ft) based on 22 pumping tests, whereas the Epler Formation is the next best aquifer in the region, with a mean specific capacity of 4.3 lps/m (21 gpm/ft) and a median specific capacity of 0.1 lps/m (0.50 gpm/ft) based on 50 tests (Meisler and Becher, 1971).

The Cocalico Formation is described as a blue, green, or purple fissile shale, with a dark blue crinoidal limestone at its base, just above the contact with the Beekmantown limestones (Jonas and Stose, 1926). It is correlative with the Martinsburg Formation that is present in other parts of southeastern Pennsylvania (Poth, 1977). The specific capacities for the three available tests on this formation are 0.1, 0.2, and 1.5 lps/m (0.58, 1.0, and 7.4 gpm/ft, respectively) (Poth, 1977).

Hydrogeology

Groundwater in the carbonate formations of Lancaster County occurs almost entirely in secondary porosity (openings along bedding and cleavage planes), and in the joints and faults resulting from the region's complex structural history (Meisler and Becher, 1971). In some areas, these openings have been enlarged by solution, which enables larger quantities of water to be stored in the formation. The degree to which these solution openings have been enlarged, and the interconnectedness of these openings determines the ability of the formation to store and transmit water (Meisler and Becher, 1971). Although the Stonehenge and Epler Formations are two of the best aquifers in the county, there are no records of caves or large conduit systems in the immediate area. There are a number of sinkholes in the area, according to a map compiled by Kochanov (1990), on which are plotted numerous sinkholes and depressions in the area around Nolte Spring. The groundwater basin for Nolte Spring is therefore most likely a fracture flow system, consisting of small conduits and solutionally-enlarged fractures.

Site History

Nolte Spring has been managed by the West Earl Township Water Authority since 1958. It was the community drinking water supply for the township until 1992, when it was determined that water from the spring did not meet turbidity criteria under EPA's Safe Drinking Water Act. The spring was replaced as a public water supply source by a well located approximately 180 meters northwest of the spring and water purchased from Lancaster City. Monitoring results obtained by the Pennsylvania Department of Environmental Protection (John Diehl, PADEP, personal comm., 1992)

following a storm in June 1992 indicate a rise in turbidity within 18 to 24 hours following the beginning of the storm, but only three measurements were collected during the course of the storm. Although Nolte Spring is no longer used as a community water supply, the former pump house and water treatment plant built over and around the spring has been maintained as the West Earl Water Works, a water treatment plant and metering station for the water from the Nolte Well and from Lancaster City (Figure 1-10). The West Earl Township Water Authority granted access to the spring for this study.

Figure 1-10. The West Earl Water Works. This building was constructed over Nolte Spring in 1958, when the spring became the community water supply for West Earl Township.

CHAPTER 2
METHODS

The following chapter describes the sampling and analytical methods used in this study. The field program included the use of continuously logging sensors and an automatic sampler as well as regular site visits to take hand-collected measurements and collect samples. Sample collection and data analysis were used in two types of monitoring: seasonal monitoring, to determine the existence and nature of temporal trends, and storm monitoring, to examine the antecedent conditions and water quality changes in the spring associated with a storm event. This chapter also describes the analytical methods as part of the storm and seasonal monitoring programs, which included analysis of major ions and suspended sediment.

Monitoring Equipment

Dataloggers were installed to continuously log water level, conductivity, turbidity, and temperature. A Global Water GL400 logger (Figure 2-1) was programmed to record water level and conductivity every 20 minutes and a HOBO H6 temperature logger (Figure 2-2) was programmed to record the temperature every 30 minutes. Early in the monitoring period, an attempt to collect turbidity measurements was made using a Global Water sensor and datalogger; however, after a series of malfunctions, the turbidity sensor was returned to the manufacturer. Both the Global Water and HOBO sensors were placed just inside the spring mouth (Figure 2-3). The Global Water sensors were wired to a waterproof data logger with a port for connection to a laptop PC or handheld computing device, such as a Palm Pilot™. The HOBO sensor contained a data logger in the sensor housing, which was placed in a waterproof container and weighted to keep it in the

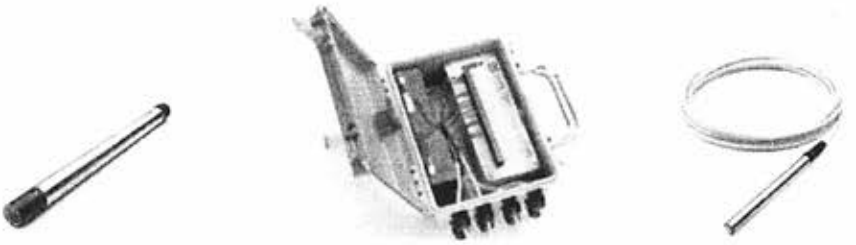

Figure 2-1. Global Water™ datalogger with conductivity sensor and transducer.

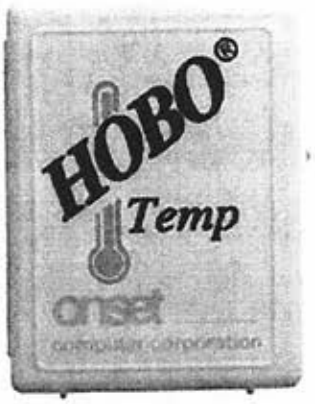

Figure 2-2. HOBO™ temperature logger with watertight container.

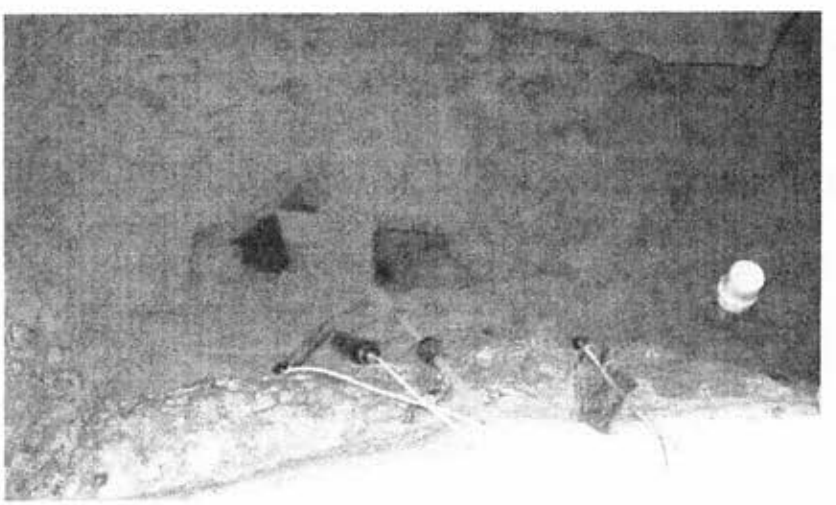

Figure 2-3. Placement of sensors in spring mouth. From left to right, conductivity sensor, turbidity sensor (removed), pump intake for automatic sampler, transducer and HOBO (in watertight container).

spring. I obtained the stored temperature data by connecting the PC or handheld directly to the HOBO.

During site visits, I uploaded the field data from the dataloggers by connecting them to a laptop PC or handheld computing device equipped with software compatible with the logger (Figure 2-4). The software for each logger enabled the user to program and deploy the loggers, as well as upload data to a file on the laptop or handheld unit and erase uploaded data from the logger. Using the laptop, I was able to export the data files to Microsoft Excel spreadsheets and view plots of the data in the field. The handheld device was connected to a PC after returning from the field, where the data was exported into Excel and viewed.

In addition to data uploads, some general maintenance was performed on the loggers and associated sensors on a regular basis at the field sites. The HOBO sensor required very little maintenance except for when it became wet, in which case the battery was replaced, and the circuitry was air dried until the next site visit, when it was launched and deployed again. The turbidity sensor at Nolte Spring was removed in the fall of 2003 after it was determined that it was not recording reliable data. The Global Water data logger also required periodic calibration and battery replacement. The Global Water data logger runs on a lead-zinc battery with a voltage of up to 13.5V. During each site visit, the voltage of this battery was checked with a voltmeter and changed if the voltage was less than 12 volts.

An ISCO 3700 automatic sampler was installed in Nolte Spring to collect water samples during the water-level rise following a storm event (Figure 2-5). Water samples collected by the automatic sampler were used for storm monitoring. The sampler was equipped with an actuator designed to turn on the sampler when the water level rose, with the sensor set between 2 and 10 cm above the water level at the time of programming, depending on how large of a storm I hoped to characterize. The sampler was programmed to collect twenty-four 800-1000 mL samples in cleaned 1000-mL HDPE bottles. The sample interval was initially programmed to be one hour, which was extended to one and a half hours after it was determined in late spring of 2003 that the storm pulse and recovery period was longer than 24 hours.

Starting in late summer of 2003, I experimented with alternate configurations for the sampler at Nolte Spring. In September 2003, two ISCO samplers were installed at the site. The actuator for the second ISCO was set approximately 10 centimeters above the actuator for the first, so that if the first sampler was triggered by a small storm, the second sampler could collect a subsequent larger storm. Alternately, if a large storm occurred initially, the first sampler would start in the beginning of the storm, and the second would start sometime in the middle of the storm, thus creating duplicate samples and extending the sampling period for the storm event. This setup was used for two storms. Starting in December 2003, the sampler was programmed for non-uniform sample intervals, starting with hourly samples for the first 12 hours of the storm, every hour and a half for the next nine hours, and every two hours for the last 12 hours of the sampling event.

Figure 2-4. Uploading of data from Global Water™ logger to a laptop in the field. Cecilia Meijas, a Temple University student worker, is shown in this photograph.

Figure 2-5. ISCO™ automatic samplers at Nolte Spring.

In addition to replacing filled bottles with empty ones, maintenance on the ISCO samplers included cleaning of the metal tip on the water level sensor, which at Nolte Spring frequently became encrusted with a calcium carbonate precipitate, and changing the pump tubing and battery. The pump tubing requires changing annually if the ISCO is used regularly, and the battery, a 13.5V lead-zinc cell, generally needed replacement with a charged battery every 2-3 weeks, regardless of whether the ISCO sampled.

Site Visits

Visits to Nolte Spring began in July 2002. The visits were generally performed on a bi-weekly basis, but the frequency of the site visits was reduced to monthly during the months of November and December 2002, and January, and February 2003, when I expected storm activity to be at a seasonal low. The site visits were used to perform general maintenance on all the equipment installed at the site, which is described above. Additionally, I collected samples and measured pH, temperature, conductivity, flow, stage and the height of the actuator above the water surface (Figure 2-6). Measurements of pH, temperature, and conductivity were obtained using a calibrated Horiba U-10 multi-parameter meter (Figure 2-7), which was placed inside the spring mouth or as close to it as possible. Flow at the spring mouth was measured at Nolte Spring was measured using an impeller stick attached to a digital counter (Figure 2-8). The count was then converted into flow as m/s using the following equation:

$$Q = C * 0.000854 + 0.05$$

where C is the counts per minute read directly from the digital display on the flow meter.

Figure 2-6. Tasks performed during site visits. These included (a) measurements of field parameters with a multimeter, (b) sample collection, and (c) measurement of spring stage.

Figure 2-7. Horiba™ U-10 multiparameter water quality meter.

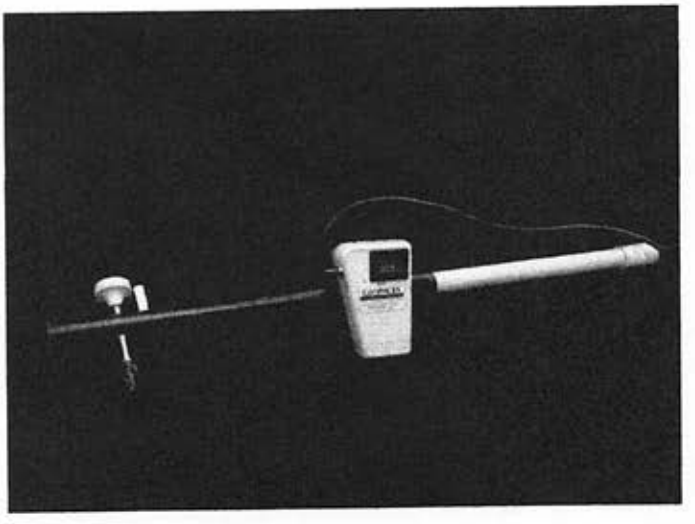

Figure 2-8. Geopacks™ flow meter.

Measurements of the water level in the spring in relation to the spring mouth, the bottom of the transducer, and the ISCO actuator were obtained using a weighted epoxy-coated stainless steel measuring tape with metric and engineering scales. For measurements of total water depth from the spring mouth to the surface, the bottom of the tape was positioned on a rock in the center of the spring mouth and the tape was held taut while the measurement at the water surface was read from the metric side of the tape (Figure 2-9).

Data obtained from the samples that were hand-collected during the site visits were used for seasonal monitoring of Nolte Spring. The samples were collected using a Masterflex peristaltic pump or a Nalgene hand vacuum pump with dedicated tubing and cleaned Nalgene™ HDPE bottles. The end of the tubing was inserted into the spring mouth when flow conditions permitted. During periods of higher flow, the end of the tubing would be placed as close to the spring mouth as possible. Suspended sediment samples were collected in 500-mL bottles, samples for alkalinity (as HCO_3^-) in 125-mL bottles, and major ions in 60-mL bottles (Figure 2-10). Geochemical samples were collected with minimal headspace in the bottles. Alkalinity samples were field filtered starting with the June 18, 2003 sample, and major ions were field-filtered starting July 28, 2003. Duplicate samples for each parameter were collected every 3 to 5 visits.

Laboratory Analysis of Samples

After samples were collected from the spring, they were transported to Temple University and stored in a refrigerator before being analyzed in the Temple University Department of Geology laboratories. Concentrations of major ions (excluding alkalinity) were measured using a Dionex ion chromatograph (Figure 2-11). Alkalinity samples

Figure 2-9. Taking stage measurements in the spring.

Figure 2-10. Sample bottles used. From right to left, 500-mL, 125-mL, and 60-mL HDPE bottles.

Figure 2-11. Dionex™ ion chromatograph. Temple student worker Kathy Gross is shown performing a dissolved ion analysis.

were titrated with H_2SO_4, using a calibrated IQ Scientific Instruments model IQ1050 ISFET solid-state pH probe to monitor pH during titration. The charge balance of dissolved ions in each sample was checked after the analyses for cations and anions had been completed. Ion balances for which the error was greater than 10 percent were investigated and if possible, the sample was rerun if no data entry errors existed. Data used for geochemical modeling had an ion balance of <5 percent, although some samples with a balance between 5 and 10 percent were used for selected plots.

Suspended sediment concentrations were analyzed by progressively filtering the sample water through 5.0 μm and 0.45 μm Millipore mixed-cellulose membrane filters, using cleaned Millipore™ glass filtering equipment and a vacuum pump (Figure 2-12). The filters were air-dried in a petri dish, and then weighed in order to determine the total mass of the sediment. This mass was then divided by the total volume of water filtered in order to obtain the concentration of suspended sediment in the sample.

Bottles filled by the automatic sampler were capped during the site visit and transported to Temple University for analysis of major cations and suspended sediment. Prior to sediment filtering, the sample was vigorously shaken and a small volume was poured off into a 60-mL HDPE bottle for cation analysis (to be reported elsewhere). Storm samples were analyzed for suspended sediment and major cations by the methods described in the previous two paragraphs.

The sediment-filtering process is extremely labor intensive and needs to be completed quickly during the seasons when storm activity is high due to the large volume of samples generated. In the interest of efficiency, between 10 and 20 bottles of a given

storm were analyzed from the 24 collected. This was determined to be a sufficient number of samples to produce a trend in sediment concentrations over the course of a storm. In order to determine an overall trend in sediment concentrations during the storm, bottles 1, 6, 12, 18 and 24 were filtered first. These data were then plotted and examined for potential peaks, and the samples that bracketed these potential peaks were included in the next round of samples to be filtered. This process was repeated until the lowest and highest sediment concentrations of the storm were determined, and all peaks were as clearly defined based on the sampling interval programmed into the ISCO prior to the storm.

Some sediment samples were chosen for further analysis by scanning electron microscope and energy-dispersive spectroscopy (SEM/EDS), and/or x-ray diffraction (XRD) if there was sufficient crystalline material in the sample. Both the SEM/EDS and XRD analyses were performed in the Materials Characterization Laboratory at Penn State University. The SEM/EDS analysis was performed to determine the shape of the sediment particles, clues to minerals and organics, and to identify the primary elements in the sample. XRD was used to confirm the presence of minerals in the sample, such as calcite, quartz, and clay minerals.

I attempted to analyze some liquid samples for particle size distribution through sediment weight percentages using a MicroTrac™ diffracted light particle size analyzer. No conclusive data could be obtained due to the small size of the sediment particles in the sample and the generally low sediment concentrations, so particle size distribution was removed from the list of analyses.

Data Reduction

Logger Data

Further data processing of the measurements from the dataloggers included conversion of the transducer measurements to measurements of stage (total depth from the datum at the spring mouth to the surface) using the hand-measured stage from the datum at the spring mouth to the water surface (Figure 2-13). First, the measurements from the transducer in feet were converted to centimeters. Next, the last transducer measurement of the data record was subtracted from the total depth (it is estimated that this measurements and the hand measurement were typically taken within 30 minutes of each other). The difference between these two values is the correction factor, C_f, which was added to all preceding transducer measurements in the data record, up to the first measurement recorded since the last uploading.

Every three months the data records were combined into seasonal summaries. Precipitation data recorded at the Lancaster Airport weather station, located approximately 7.5 km west of Nolte Spring, were downloaded from the National Oceanic and Atmospheric Agency (NOAA)'s National Climatic Data Center (NCDC) website, https://www.ncdc.noaa.gov/oa/ncdc.html. This dataset included unedited hourly and daily precipitation, as well as daily weather observations. The daily precipitation record was added to the seasonal summaries of stage and conductivity.

Stage and Velocity

Most of the data processing involving stage has been described in the logger section of this chapter. By combining the stage data, the velocity measured in the spring mouth

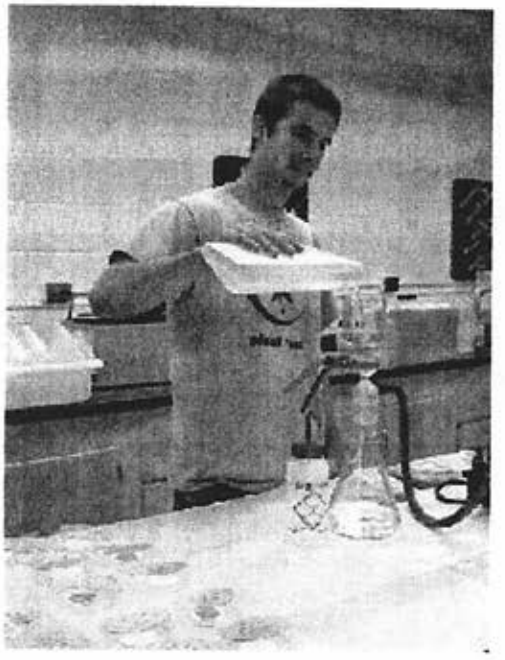

Figure 2-12. Laboratory setup for sediment filtering of samples. Temple student worker Stephen Scott is shown filtering a spring sample.

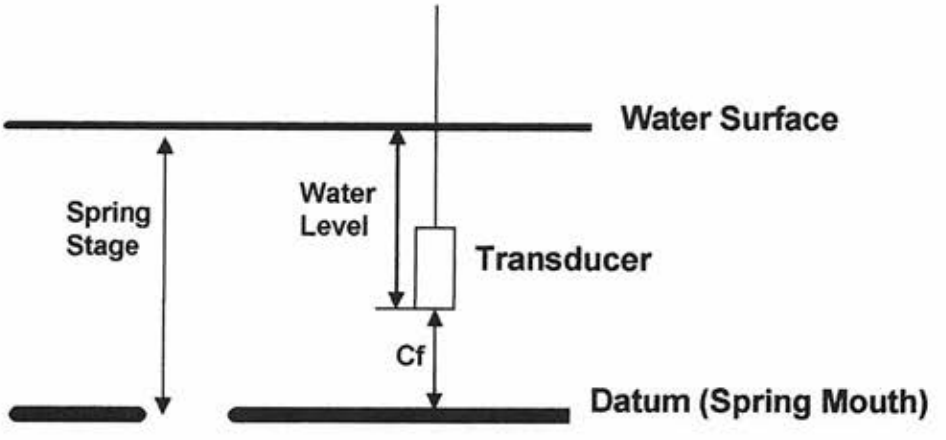

Figure 2-13. Measurements used for correction of transducer measurements. Cf is the correction factor used to obtain spring stage.

with the impeller stick, and the cross-sectional area of the spring mouth, which is approximately 162 cm^2, I calculated discharge values for the site visits in liters per second, L/s. Using these measurements, I constructed a stage-discharge curve, which was necessary to estimate the size of the groundwater basin, or capture zone, for the spring.

Geochemical Data

Hardness was calculated using the dissolved Ca^{2+} and Mg^{2+} concentrations and the ratio of the formula weight of $CaCO_3$ to the atomic weights of the respective ions in the equation H = 2.5*[Ca] + 4.1*[Mg] from Freeze and Cherry (1979). SI_C and P_{CO2} values for Nolte Spring were calculated using the United States Geological Survey geochemical modeling software PHREEQC (Parkhurst, 1999). The SI is used in carbonate waters to quantify their deviation from equilibrium with calcite or dolomite. For calcite, the SI_C is defined as

$$SI_C = \log \frac{a_{Ca^{2+}} \cdot a_{CO_3^{2-}}}{K_C}$$

where the numerator of the logarithm describes the ion activity product (IAP) for the dissociation of calcite, and K_C is the solubility product constant for calcite. An SI_C of 0 indicates that the water is in equilibrium with calcite, an $SI_C < 0$ means that the water is undersaturated with respect to calcite, and an $SI_C > 0$ indicates supersaturation with respect to calcite. Because reactions involving dissolution or precipitation calcite are kinetically inhibited, these values alone cannot be used to predict the presence or absence of solid calcite in carbonate waters.

P_{CO2} is the partial pressure of carbon dioxide in a gas phase in equilibrium with the water being sampled. It can be calculated from

$$P_{CO_2} = \frac{a_{HCO_3^-} a_{H^+}}{K_1 K_{CO_2}}$$

where K_1 is the first dissociation for carbonic acid (H_2CO_3), and K_{CO2} is the equilibrium constant for dissolution of carbon dioxide in water to form carbonic acid. P_{CO2} values for samples from Nolte Spring were calculated with PHREEQC using the alkalinity analyzed in the laboratory from samples collected during site visits and the field-measured pH at the time of sampling.

Sediment Data

Determination of sediment concentration using the mass of the sediment on the filter and the mass of the water filtered have been described in a previous section of this chapter. For quality assurance purposes, duplicate sediment samples were collected and run for approximately 20% of the samples. Data from duplicate sediment samples indicated an error of about ±1 mg/L.

In addition to sediment concentration, sediment flux was calculated from the discharge measurements obtained during site visits and the sediment concentration of the samples collected at that time. Sediment flux is defined as the mass of sediment flowing through a cross-sectional area over a specified period of time. In this case, I assumed a one hour period, and multiplied the sediment concentration by the converted discharge to obtain mg/H of sediment through the spring mouth.

CHAPTER 3
CAPTURE ZONE ANALYSIS

Introduction

Published information was not available regarding the regional groundwater flow for the area in which Nolte Spring is located and the groundwater basin for Nolte Spring, so I estimated a general direction of groundwater flow and estimated the size and orientation of the capture zone for the spring using existing data. This information is important for a number of reasons. Identification of regional flow patterns can provide clues to different groundwater flow systems within a basin. In Chapter 4, the possibility of a deep circulation system of very old water is discussed. Such large regional flow systems can sometimes be identified by an analysis of flow patterns over a large area. Also, an understanding of the type of rocks through which the groundwater flows en route to the spring can be used to determine recharge areas, and may identify potential sources for geochemical variability in the spring. From a groundwater protection standpoint, regional hydrogeologic data are particularly necessary in delineating protection areas for springs and wells that serve as community drinking water supplies.

Regional Groundwater Flow

To determine groundwater heads in the area around Nolte Spring, well records from West Earl Township (the municipality in which Nolte Spring is located) and adjoining municipalities were obtained from the Pennsylvania Ground-Water Information System (PaGWIS) (Moore, 1998), a database of well records compiled by PADEP that includes copies of USGS records for wells in Pennsylvania. Only wells completed in the

Epler and Stonehenge Formation were selected from those located in West Earl and adjoining municipalities.

Plotting the well locations and groundwater elevations on a topographic map of the area showed that there are only six wells listed in the PaGWIS database for the basin around Nolte Spring. Most of these wells are close to the Conestoga River, so the groundwater heads in these wells are heavily influenced by the level of the river, and there was not sufficient distribution for contouring water levels. Based on the local topography, a rough approximation of regional groundwater flow direction in northeast Lancaster County is south, toward the Conestoga River.

More detailed groundwater flow directions in karst are hard to predict because of the heterogeneity inherent in karst aquifers, which is based on the degree of karst development and the geometry of the conduit network. Furthermore, karst conduits do not necessarily flow in the same direction as the potentiometric surface, and tracer tests may be needed to determine the direction(s) in which the water is most likely to flow.

Capture Zone

The capture zone, or the surface and groundwater area from which water flows to Nolte Spring, was estimated using Rules of Thumb (RTs), guidelines provided by the United States Environmental Protection Agency (USEPA) for determining the contributing area around drinking water sources supplied by groundwater, such as wells and springs (Ginsberg and Palmer, 2002). These guidelines are provided so that groundwater professionals and communities can identify sources of potential contamination and assess the susceptibility of the well or spring to contamination by

those sources. A fixed-radius method is often used by states to delineate source water protection areas, but this is not an effective method for karst aquifers, because many assumptions of this approach, such as a porous-medium aquifer, and that groundwater flows equally from all directions, do not apply to karst.

In addition to groundwater protection, information on the type of rocks groundwater flows through before it is discharged through the spring contributes to a greater understanding of the geochemical and sedimentologic variations in spring discharge, based on the pathways through which water travels to the spring. Knowledge of the spring's capture zone combined with local geology can be used to determine the recharge area and to identify whether potential surface-water entry points, such as sinkholes and sinking streams contribute to the discharge from a particular spring. The length and orientation of potential flow paths to the spring can also be estimated from the capture zone. The capture zone can influence spring response to storms.

Method for Calculation

The RTs provide information on how to estimate a spring's capture zone from hydrogeologic data, including discharge values for the spring, discharge of the stream or river into which the spring flows, and the strike and dip of bedding in the aquifer. To calculate the capture zone area according to the RTs, stream discharge was used to estimate the recharge rate for the region. The discharge per unit area for the river or stream must be calculated by dividing the discharge by the drainage basin area, which is 839 km^2 for the Conestoga River. The RT method assumes the rate at the river applies also to the spring. The spring discharge is then divided by the discharge per unit area, in

order to determine the area of the capture zone necessary to supply the spring discharge. Methods for the calculation of discharge values for Nolte Spring have been described in Chapter 2. The highest baseflow discharge for the spring is recommended by the RTs, because it results in the most conservative (largest) capture zone area. I used a number of spring discharge measurements because I performed this calculation to determine the sensitivity of the capture zone area to changes in spring discharge, rather than for contamination risk assessment purposes.

When applied to estimations of the capture zone area, however, the discharge calculated from impeller velocity measurements resulted in a capture zone area not much bigger than the building over the spring (500 m^2), which is not physically reasonable. Furthermore, the discharge values based on these velocities do not mach observed spring discharge rates. Nonetheless, the impeller velocities showed a trend between velocity and stage, as expected (Figure 3-1). A correction factor was needed to obtain a more accurate velocity at the spring.

A flow rate of 21.9 L/s on March 4, 2004 was measured at the outflow pipe which discharges from the west wall of the building housing the spring by measuring velocity directly using the travel time of a sponge through the pipe. The length and diameter of the pipe were obtained from building plans on file in the spring building. However, this was the only measurement taken from the outflow pipe. The stage at this time was 119.9 cm. The stage can be correlated to a typical (low) impeller estimate of discharge. To relate stage to impeller discharge, a trend line was used rather than raw data, which was noisy. I fitted a trend line to the upper range of the stage-discharge curve (Figure 3-2)

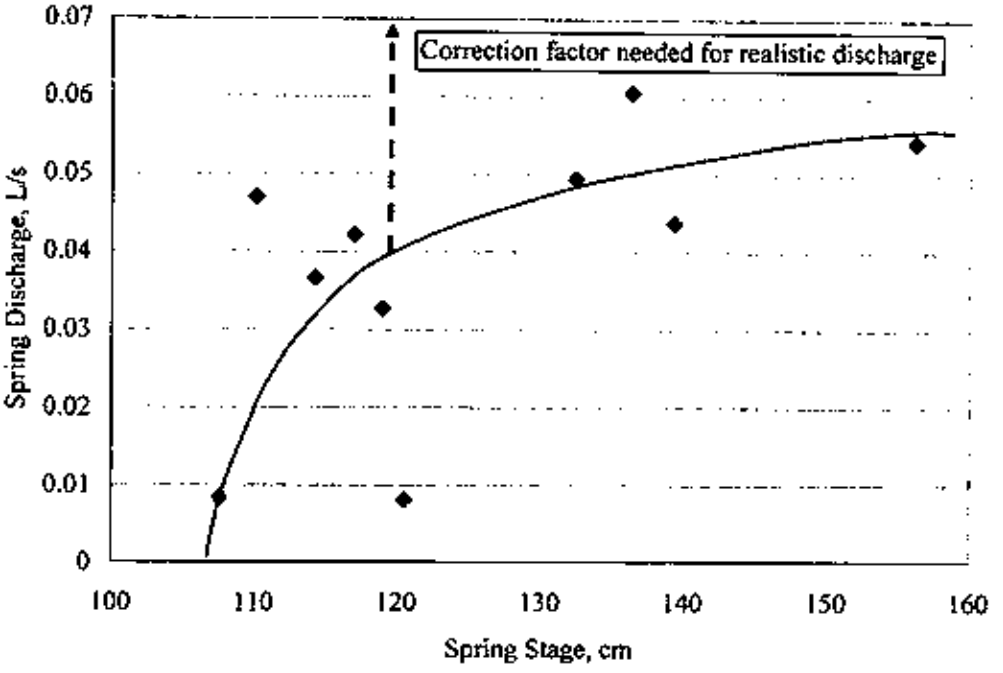

Figure 3-1. Stage-discharge curve calculated from impeller measurements in the spring. Used in the capture zone area estimation, these values proved to be too small to result in a reasonable size for Nolte Spring's capture zone, so a correction factor was needed (see text).

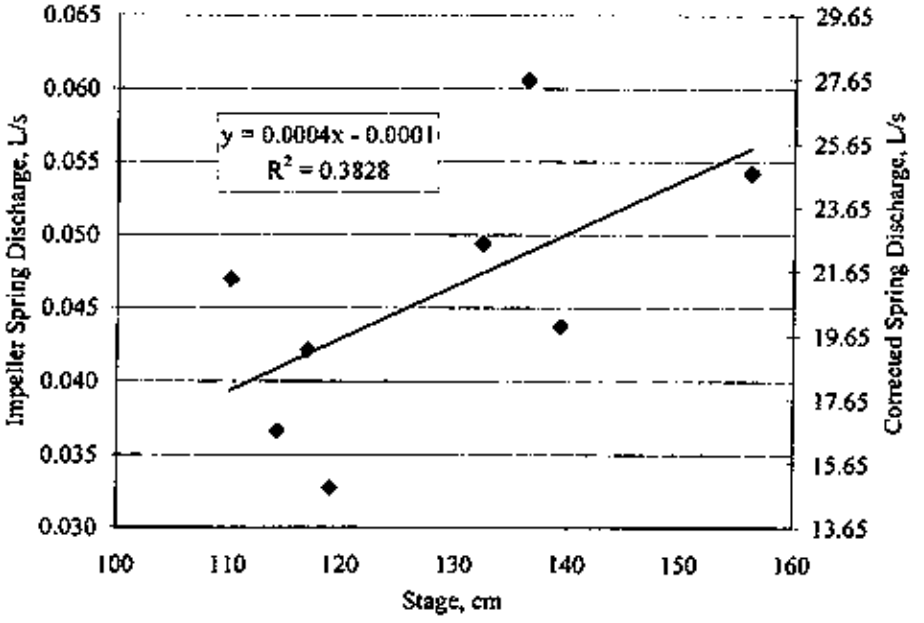

Figure 3-2. Trendline and equation for upper part of stage-discharge curve. The equation was used to interpolate a corresponding spring mouth discharge for the outflow pipe measurement on March 4, 2004.

constructed from the discharge values calculated from the impeller measurements because these values represent most of the typical conditions of the spring and the upper range of this curve was linear. I used the equation of the trend line,

$$y = 0.0004x + 0.0001$$

where x is stage, in cm, and y is to interpolate a "spring mouth" impeller flow measurement for the March 4, 2004 outflow pipe measurement. Now the true discharge could be compared to values estimated from the impeller. I divided the outflow pipe measurement by this interpolated spring mouth measurement, obtaining a ratio of 455.6. Each of the impeller discharge values was multiplied by this ratio to approximate what the outflow pipe discharge was in the spring mouth (Table 3-1). These new discharge values, although rough, were closer to observed discharge and resulted in larger and more reasonable capture zone area calculations. Impeller measurements taken on October 31, 2002 and August 22, 2003, were excluded from this estimation because they were not in the linear part of the stage-discharge curve. When a better stage-discharge relationship is obtained (included in future work planned at the study spring) the non-linear portion could also be included.

The estimated spring discharge values and the corresponding stream discharge for the date the spring was measured were used to see how changes in spring discharge affect the capture zone (Table 3-2). These dates cover the typical range in the spring during the study period, excluding flood and drought extremes. I obtained stream discharge data for the Conestoga River at Lancaster, United States Geological Survey (USGS) gauging station 01576500, located approximately 11 km southeast of Nolte Spring, in the

Table 3-1. Pipe Flow Rates Estimated from Impeller Measurements

Date	Stage (cm)	Impeller discharge (L/s)	Pipe Discharge (L/s)	Pipe-Impeller Conversion
10/17/2002	119.0	0.033	14.90	
11/21/2002	139.3	0.044	19.92	
12/20/2002	156.2	0.054	24.72	
2/5/2003	117.0	0.042	19.18	
5/29/2003	110.1	0.047	21.40	
6/18/2003	132.4	0.049	22.50	
7/9/2003	136.3	0.061	27.59	
9/5/2003	114.3	0.037	16.67	
3/4/2004	119.9	0.048	21.86[1]	455[2]

[1] Discharge measured at outflow pipe on 3/4/04

[2] Correction factor for impeller measurements, 21.86/0.048

Table 3-2. Discharge Values Used for Capture Zone Calculations

Date	Spring Discharge[1] L/s	Stream Discharge[2] L/s	Discharge/ Unit Area[3] L/s/km^2	Capture Zone[4] km^2
10/17/2002	14.90	52953	63.10	0.2
11/21/2002	19.92	18434	21.97	0.9
12/20/2002	24.72	23163	27.60	0.9
2/5/2003	19.18	14470	17.24	1.1
5/29/2003	21.40	12629	15.05	1.4
6/18/2003	22.50	15801	18.83	1.2
7/9/2003	27.59	12573	14.98	1.8
9/5/2003	16.67	14073	16.77	1.0
3/4/2004	21.86	11780	14.04	1.6

[1] From Table 3-1 (pipe flow estimated from impeller data)

[2] From USGS gauging station 01576500

[3] Stream discharge/839 km^2

[4] Spring discharge/Discharge/Unit Area
(column 1/column 3)

Conestoga Formation, which is also composed of carbonates. Data were available from the USGS National Water Information System (NWIS) website, at http://water.usgs.gov/nwis/sw.

For the geologic information, I used a geologic map of Lancaster County (Poth, 1977) and a sinkhole map prepared by Kochanov (1990). Using these maps, I obtained an estimation of the strike orientation and dip. The average strike of the beds in the area is approximately N69°E and they dip shallowly at an angle of 2-3° to the northwest (Rick Valentino, Department of Geology, Temple University, personal communication, 2004). For one of the lateral boundaries of the capture zone I drew a line from the spring along the dip to the northwest until it intersected surface elevation. The RTs recommend drawing this line in the updip direction, which would be to the southeast, but the Conestoga River is located immediately south of the spring, and the RTs also state that the capture zone cannot cross a perennial stream. Because the dip angle indicates that the bedding is almost flat in this area, I drew the capture zone's lateral boundary in the downdip direction, thus avoiding any perennial streams. For the downdip boundary of the capture zone, I drew a line from the spring parallel to strike into the karst area that feeds the spring. This area was identified by the recharge features marked on the sinkhole map, and there is a perennial stream located to the southeast of the spring, into which the spring discharge flows. The capture zone area calculated from the spring and stream discharge was used to complete delineation of the capture zone, which roughly formed a quadrilateral.

If the karst aquifer for the spring is dominantly fractured rather than dominantly bedded, it is recommended that an area roughly one-half the size of the capture zone be added to the downdip boundary of the capture zone, as the groundwater in conduits often flows independent of the strike of the bedding (Ginsberg and Palmer, 2002). Based on rapid storm response and variability in geochemical data (see Chapters 4 and 5) I believe that there may be some fractures or weakly developed conduits in the karst aquifer for Nolte Spring. I added the area for conduit flow between the southern boundary of the capture zone and the Conestoga River, observing the specification in the RTs to avoid perennial streams when delineating the capture zone. The RTs suggest half the width be added based on observations from other karst sites in fracture-dominated aquifers.

Results of Capture Zone Area Estimation

The total area of the capture zone calculated for Nolte Spring, with the conduit-flow component included, ranged between 0.2 and 1.8 km^2 over the range of values for discharge measured in the spring (Table 3-2). The capture zone extends north and east of the spring, where the Conestoga River is the southern boundary for the conduit-flow component of the capture zone (Figure 3-3). A number of sinkholes and topographic depressions which may be buried sinkholes have been identified within the capture zone (Kochanov, 1990), which indicates that there is a high potential for surface water to enter the karst system directly. The capture zone lies within both the Epler and Stonehenge Formations. As mentioned in Chapter 1, the Stonehenge Formation is the most productive aquifer in Lancaster County, so there may be larger conduits within this formation, and faster groundwater flow. The presence of two different formations, with

dissimilar hydrogeologic properties, within the capture zone for Nolte Spring indicates that there may be different hydrogeologic pathways to the spring within the capture zone.

CHAPTER 4
CONTINUOUS MONITORING

Introduction

As mentioned in a previous chapter, logging sensors were installed in the spring mouth at Nolte Spring, collecting measurements of water level and conductivity at 20-minute intervals, and temperature at 30-minute intervals. Continuous monitoring of stage, temperature and conductivity was performed to examine both the short- and long-term variability in the chemical and hydrologic characteristics in the spring. These data helped to interpolate between data points from samples collected during site visits, and provided high-resolution information about how the spring discharge changes during storms. These storm data were especially useful for storms that the automatic sampler missed.

For the purpose of organizing the significant amount of logger data collected over the monitoring period, which lasted from mid-July 2002 until the end of December 2003, the convention of separating the monitoring period into seasons was adopted. The Summer 2002 and Summer 2003 seasons included the months July, August and September of the respective years; the Fall 2002 and Fall 2003 seasons included the months of October, November and December; February and March were included in the Winter 2003 season (there was no logger data from January, this is explained below); and the Spring 2003 season consisted of the months of April, May and June. The divisions were adopted for ease of plotting and organization, but similar patterns were observed within each season. The data are presented below with this seasonal organization, in

chronological order from the Summer 2002 to Fall 2003 seasons. In this chapter, the results are presented first, followed by the interpretation (discussion).

Results

Over the monitoring period, the baseflow stage of Nolte Spring ranged from 30 cm above the spring mouth to approximately 180 cm (Figures 4-1 through 4-6). In this study, I defined baseflow as the time between storm pulses in the spring. The lowest baseflow stage in the spring was recorded in the summer of 2002, during a severe drought. The highest baseflow stage was recorded in March 2003. This measurement was taken after a late winter thaw, which occurred after significant snowfall in February 2003. Flood stage in the spring exceeded 200 cm during a storm on June 18, 2003, when the peak stage was 267 cm, and during a storm on September 23, 2003, when the peak stage reached 284 cm. Baseflow conductivity measured in Nolte spring ranged from approximately 550 µS/cm (microSiemens per centimeter), recorded on February 25, 2003 to 820 µS/cm, recorded on August 24 and 28, 2002 (Figures 4-1 through 4-6). This range does not include a storm peak of 1800 µS/cm, which occurred on September 26, 2002 and is discussed later in this chapter.

Temperature did not change significantly between seasons or in response to storms, except in the drought of 2002. During this time, from mid-July to mid-October 2002, the temperature ranged from 11.7 to 15.6°C. During the September 26, 2002 storm, the temperature fell to 11.3°C for a period of 4 days, increased briefly to 11.7°C then fell to 11.3°C during a storm on October 4, 2002, and then increased once more to

12.5°C. The spring temperature decreased to 11.3°C following a storm on October 11, 2002, then was constant at this temperature for the remainder of the study period.

Summer 2002

The monitoring period began during a severe drought, which lasted in Lancaster County from August 2001 until January 2003, when the State of Pennsylvania lifted the Drought Emergency and upgraded the status of most counties in southeastern Pennsylvania to Normal. The lowest stage recorded during the monitoring period occurred during the drought, in September 2002. Spring stage during baseflow periods in summer 2002 ranged from 25 cm to 79 cm (Figure 4-1). In response to a storm event on September 26, 2002, the stage rose from 28 cm to 92 cm over a period of 3.5 days, at an average rate of 5.6 cm per hour.

The baseflow conductivity recorded at Nolte spring during the summer of 2002 ranged from 700 - 820 µS/cm, and is the highest measured during the monitoring period (Figure 4-1). After a storm on September 26, 2002, during which 6 cm of rain fell in 37 hours, the conductivity rose from 780 µS/cm to 1708 uS/cm, then decreased to 710 µS/cm over another period of 37 hours. Other than that storm, which is discussed in more detail at the end of this chapter, the conductivity generally followed a trend of gradual increase from mid-July (beginning of monitoring period) until the September 26 storm.

Some disturbance in conductivity occurred around August 15 - August 30, concurrent with rain events that occurred on August 15 and 20 - 24. Water level in the spring rose approximately 10 cm in response to the latter storm event on August 24. A second water level rise occurred on August 29, 2003, but the weather station used for

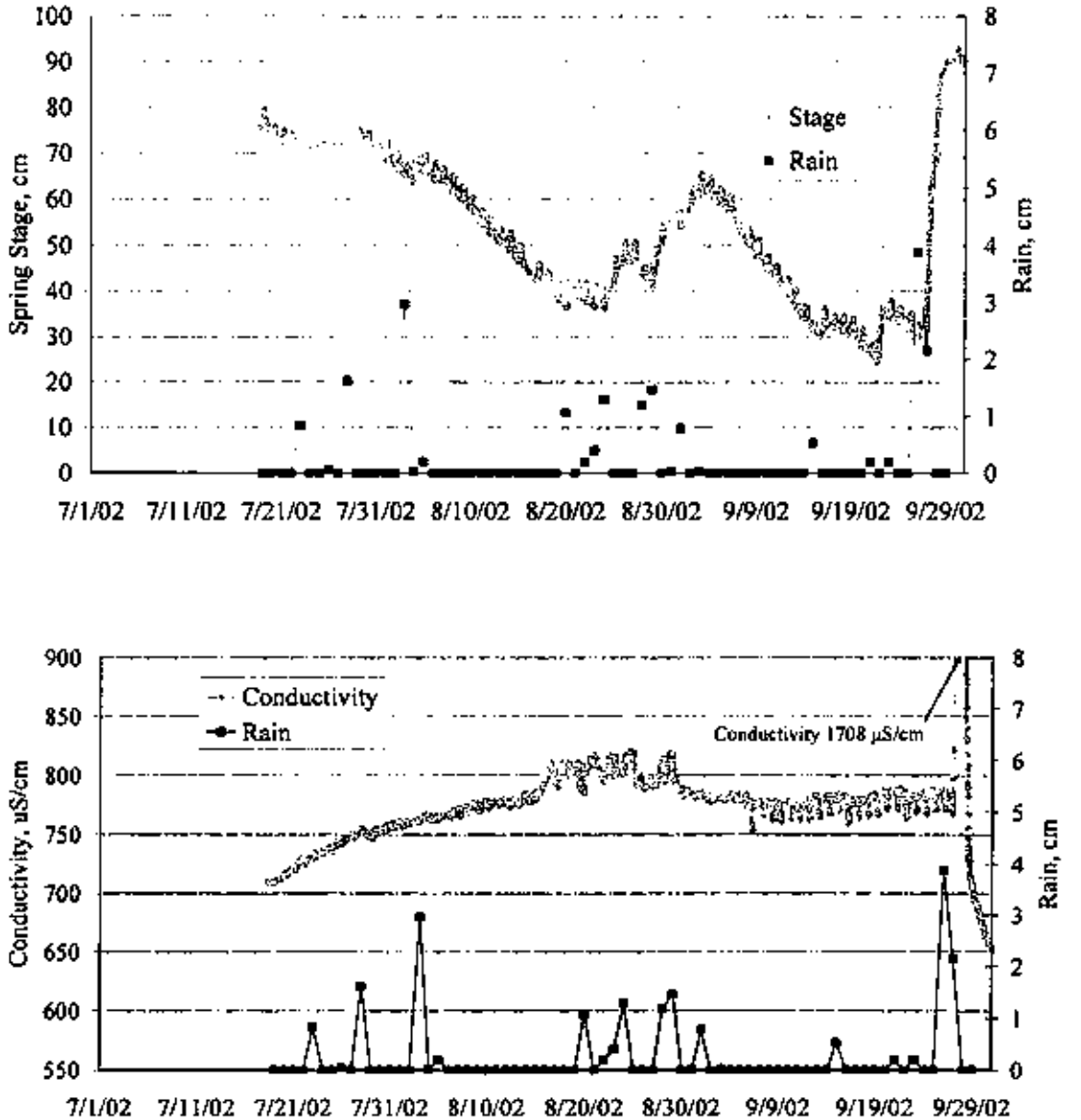

Figure 4-1. Summaries of stage and conductivity data from the Summer 2002 season. Pennsylvania was in a severe drought during this time, which resulted in the lowest stage and highest conductivity of the monitoring period.

precipitation did not record any rain for that day, so a local precipitation event may have occurred at this time.

Fall 2002

The stage recession curve following the September 26, 2002 storm continued through the beginning of October 2002 (Figure 4-2). A water level increase occurred on October 11, concurrent with a storm event on the same day. During this water level rise, the field-calibrated range of the transducer was exceeded, so data from the period of October 11 through 21, 2002 was lost. However, a field measurement on October 17, 2002 of 119 cm was added to the data record (Figure 4-2). On October 31, the transducer was raised to record the higher stage. After October 31, 2002, the stage did not change significantly from 120 cm until a storm on November 17, 2002, in response to which the stage rose approximately 20 cm. Two small storms (<2 cm recorded precipitation) occurred during this time. The lack of spring response suggests that the precipitation was too low to affect the spring, or that the rain events were localized to the weather station.

After the September 26 storm, the conductivity dropped to 650 µS, more than 100 µS lower than the antecedent conductivity recorded during the month leading up to the storm (Figure 4-2). With the exception of a storm-related disturbance on October 11, 2002, this is the lowest conductivity measured during fall 2002, with the highest recorded approximately 700 µS/cm. The only conductivity responses to storm events during this season occur after storms with a precipitation rate of at least 1.3 cm/day, with the more pronounced responses after storms with a precipitation rate of 2.5 cm/day or more. All conductivity responses to fall storms are a rise followed by a decrease. Of the four fall

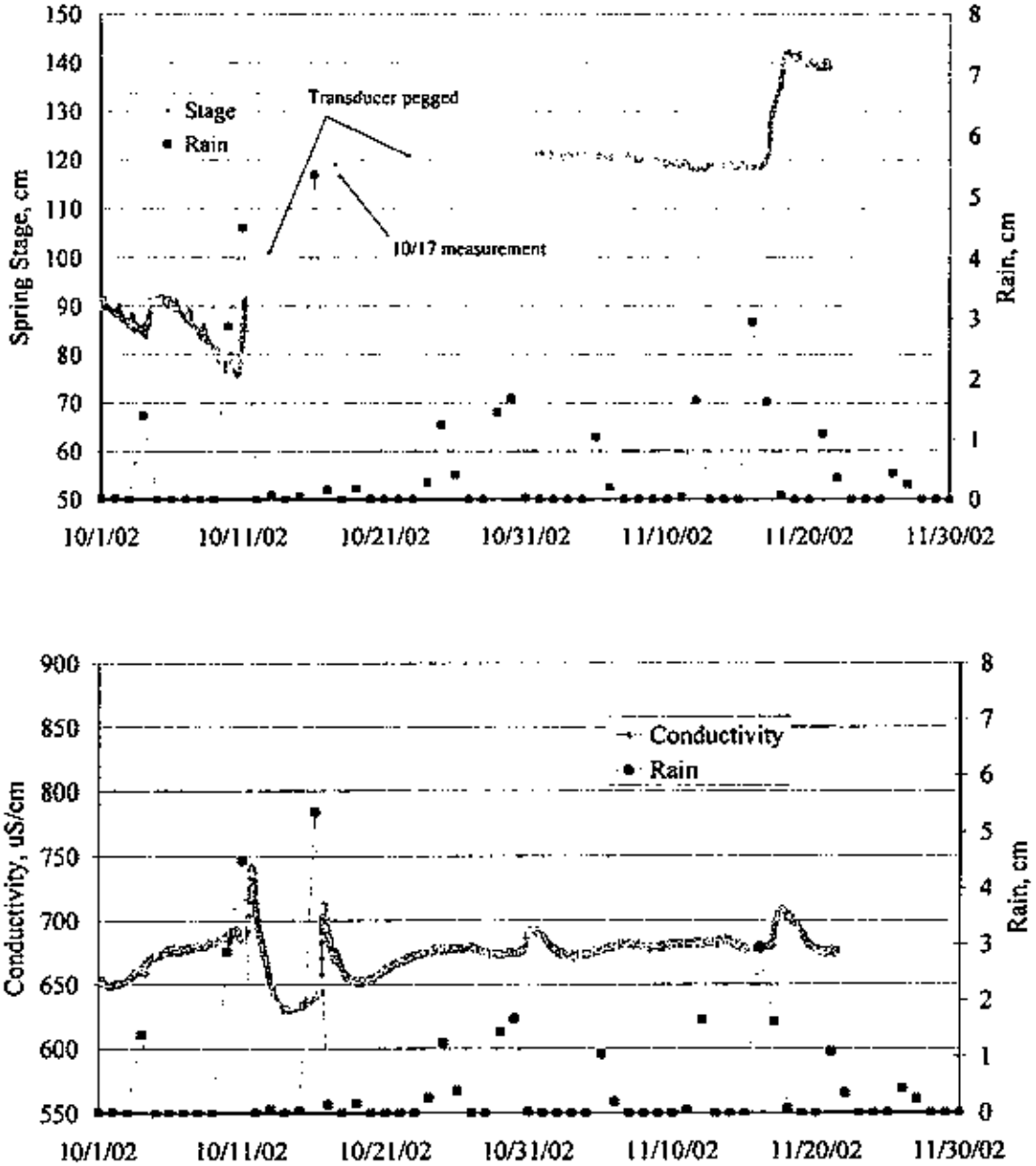

Figure 4-2. Summaries of stage and conductivity data from the Fall 2002 season. The spring began to recover from the drought following a storm on September 26, 2002, but the stage data was not recorded, because it rose above the range of the transducer after a storm on October 11.

storms that caused conductivity responses, two of the responses are steep and two are gradual. Due to a malfunction of the data logger, both the conductivity and water level data from November 22, 2002 to February 4, 2003 was lost.

Winter 2003

Starting on February 6, 2003 the stage decreased from approximately 125 cm to 105 cm, and then a combined rain and snowmelt event on February 22-24, 2003 caused the stage to rise to approximately 160 cm (Figure 4-3). This rise in stage was followed by four more increases through the first two weeks of March 2003, only two of which were accompanied by precipitation events. The water level rises in early March are thought to have been caused by air temperature rises which triggered discrete snowmelt events. During these two weeks, spring stage rose to almost 200 cm (Figure 4-3). Another stage rise, of approximately 33 cm, occurred on March 21, 2003, in response to 3.5 cm of rain, which fell on March 20.

Winter 2003 conductivity ranged between approximately 660 and 670 µS/cm until the storm/snowmelt event on February 23. At this time the conductivity decreased rapidly to the seasonal low of 550 µS/cm over a period of almost two and a half days (Figure 4-3). Immediately following this significant decrease, the conductivity started to recover, and ranged between 600 and 630 µS/cm through the rest of the season. This period of time included a series of 3 conductivity decreases between March 3 - 13, 2003, and the most intense storm of the winter on March 20, 2003, during which precipitation was approximately 3.5 cm. The conductivity response to the March 20 storm, however,

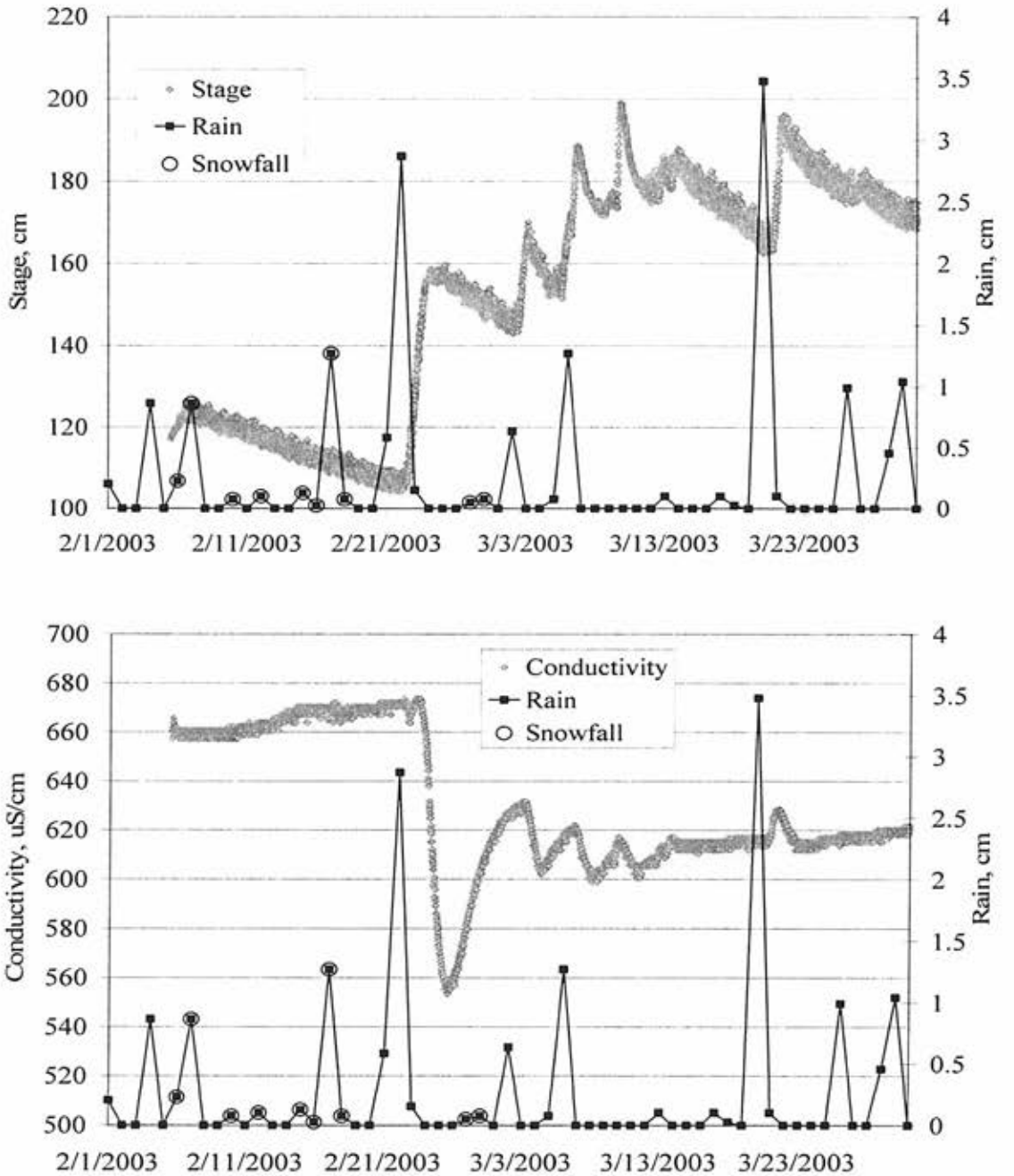

Figure 4-3. Summaries of stage and conductivity data from the Winter 2003 season. Due to significant snowmelt at the end of February and the beginning of March spring stage was high during most of March. The influx of dilute water to the karst system is thought to have caused the low conductivity values observed from the end of February through March 2003.

is only a small rise (13 uS/cm), followed by a decrease to near antecedent conductivity of approximately 615 μS/cm.

Spring 2003

The general trend in stage from April 1 through the end of May is a continuation of the recession which began in late March 2003, from high water caused by the snowmelt period in early March and the March 20 storm (Figure 4-4). Stage in the beginning of April is approximately 150 cm and the seasonal low stage occurs during the period of May 24 – 26, 2003. This recession is interrupted by a rise in stage in response to a series of small (<2.5 cm total daily) rain events which lasted from April 4 – 11, 2003, and from May 4 – 12, 2003. Except for a small water level rise during this period, there is little to no spring response to the precipitation, which may be attributed to local rain events recorded at Lancaster Airport which did not occur or had less precipitation within the capture zone for Nolte Spring. Following the seasonal low stage in May, a period of heavy rains caused the stage to increase. A particularly heavy storm on June 21, 2003, which caused the Conestoga Creek and tributaries in the area of Nolte Spring to flood, resulted in a water level rise of 133 cm in the spring over approximately 16 hours.

Conductivity in Spring 2003 ranged from approximately 620 μS/cm to 645 μS/cm, not including storm minima and maxima. Three significant conductivity responses to storm events occurred during the spring season (Figure 4-4). On May 27, 2003, after a low-intensity (0.82 cm/day) storm event lasting from May 22 to May 26, 2003, the conductivity decreased 18 μS/cm over 3 days. A higher intensity storm event (2.44 cm/day) on June 2 - 4, 2003 caused the conductivity to respond with a steep